

REVIEW OF CONTEMPORARY APPROACHES
TO FATIGUE DAMAGE ANALYSIS

by

D. F. Socie and JoDean Morrow
Department of Theoretical and Applied Mechanics

A Report of the
FRACTURE CONTROL PROGRAM

College of Engineering, University of Illinois
Urbana, Illinois 61801
December, 1976

TABLE OF CONTENTS

	<u>Page</u>
I. PURPOSE AND SCOPE	1
II. FUNDAMENTALS OF FATIGUE DAMAGE ANALYSIS	2
A. Cyclic Stress-Strain Behavior of Metals	2
B. Fatigue Properties of Metals	4
C. Cycle Counting	7
III. METHODS OF FATIGUE DAMAGE ANALYSIS	9
A. Simulation of Stress-Strain Response	9
B. Component Calibration Techniques	12
C. Notch Analysis	13
1. Neuber's Rule	13
2. Fatigue Notch Factor	16
D. Cumulative Damage Analysis	17
IV. APPLICATION OF A STRAIN BASED ANALYSIS TO THE SAE CUMULATIVE FATIGUE DAMAGE TEST PROGRAM	19
A. Review of Test Program	19
B. Nominal Strain-Life Analysis	20
C. Component Calibration Analysis	22
1. Experimental Determination of Load-Strain Curve	22
2. Finite Element Determination of Load-Strain Curve	22
3. Load-Strain Conversion and Fatigue Analysis	23
4. Load-Stress-Strain Conversion and Fatigue Analysis	24
D. Notch Analysis	25
1. Experimental Determination of the Fatigue Notch Factor	25
2. Analytical Determination of the Fatigue Notch Factor	26
3. Neuber Notch Analysis	27
V. DISCUSSION OF LIMITATIONS OF APPROACH	28
VI. COMPUTER PROGRAM LISTINGS	31
Appendix A - Nominal Strain-Life Analysis and Rainflow Counting	31
Appendix B - Load-Notch Strain Analysis	33
Appendix C - Load-Stress-Strain Analysis	35
Appendix D - Neuber Notch Analysis	37
REFERENCES	39

I. PURPOSE AND SCOPE

A review of current methods for fatigue damage analysis employing smooth specimen materials data for predicting the service life of components and structures subjected to variable loading will be presented. It is written for the beginner in this area of fatigue damage analysis rather than for experienced practitioners. Special emphasis is placed on the detailed elements of the analysis, as well as the overall pattern for synthesizing these elements into a working computer-based program.

Most of the pertinent literature in this field is less than ten years old and often difficult for the novice to locate. For this reason, key papers are cited as a guide to publications and useful data sources. Our purpose is to provide the reader with a single document containing, as nearly as possible, all the information required to implement the current state of the art damage analyses.

After discussing the details of the analysis, application of the techniques will be illustrated by making life predictions for the SAE Cumulative Fatigue Damage Test Program.

Appendices are presented with flow charts and Fortran IV listings of computer programs of all the necessary elements in a complete fatigue damage analysis for crack initiation life.

II. FUNDAMENTALS OF FATIGUE DAMAGE ANALYSIS

A. Cyclic Stress-Strain Behavior of Metals

The monotonic stress-strain curve* for metals is used to obtain design parameters for limiting stresses on structures and parts subjected to static loading. By analogy the cyclic stress-strain curve may be used by the designer to evaluate the durability of structures and parts subjected to cyclic loading. The stress-strain response of metals which are metastable under cyclic loading is usually altered due to repeated plastic strain. Depending on the initial condition of a metal (i. e. quenched and tempered, annealed, cold worked, etc.) and the test condition, it may cyclically harden, soften or remain relatively stable. The cyclic stress-strain curve can be compared with the monotonic stress-strain curve to quantitatively assess cyclically induced changes in material behavior, as shown in Fig. 1. In the case of RQC-100, it is shown that cyclic yielding occurs well below the monotonic yield. This shows the falsity of designing to a monotonic yield strength rather than using the cyclic stress-strain curve for designing structures to resist fatigue loading.

Just as the monotonic stress-strain curve relates static applied stress and the resultant static strain, the cyclic stress-strain curve relates cyclic stress and strain. Of particular importance is the amount of cyclic plastic strain, since this quantity is intimately related to fatigue damage, as will be discussed in Section II. B. An equation of the following form is generally used to express the cyclic stress-strain relationship:

$$\frac{\Delta\epsilon}{2} = \frac{\Delta\epsilon_e}{2} + \frac{\Delta\epsilon_p}{2} = \frac{\Delta\sigma}{2E} + \left(\frac{\Delta\sigma}{2K'}\right)^{1/n'} \quad (1)$$

The Δ , in the above equation, indicates completely reversed ranges of stresses and strains and subscripts e and p stand for elastic and plastic strain. The two material

*Often simply referred to as a tensile stress-strain curve.

properties, n' and K' , are the cyclic strain hardening exponent and cyclic strength coefficient, respectively. These are determined by subjecting smooth samples to completely reversed strain control, as illustrated in Figs. 2(a) and 2(b). After the transient adjustment, essentially the same size and shape of hysteresis loop will be produced cycle after cycle. The stable, steady-state loop for each specimen tested is used to obtain one point on the cyclic stress-strain curve. Enough specimens are cycled at different strain ranges to provide the stable cyclic stress-strain behavior over a sufficient range to fit a function of the form of Eq. 1 to the locus of tips of these stable loops, as shown in Fig. 3.

A number of short-cut methods for approximating the cyclic stress-strain curve from only one specimen have been suggested. Perhaps the most popular of these is the incremental step strain test, illustrated in Fig. 4. In this test one specimen is subjected to several large completely reversed strain cycles, and then the strain is gradually reduced in about forty steps to the point of zero stress and strain. The strain is then incrementally increased to the large level, then decreased, and so forth to failure. After the initial transient hardening or softening, the plot of stress versus strain furnishes an approximation to the locus of tips of stable loops. Once again an equation, of the form of Eq. 1, can be fitted to this curve. However, the reader is cautioned that the values of K' and n' obtained in this way may be somewhat different from that obtained using the companion specimen method.

For the purpose of better understanding the meaning of the cyclic stress-strain curve, it should be noted that if a sample is pulled in tension from zero stress and strain after incremental step straining, the stress-strain curve that is obtained will be very much like the stable cyclic stress-strain curve. This is illustrated in Fig. 5. Once again the reader is cautioned that the values of n' and K' obtained from a tension test after incremental step straining may be somewhat different than those obtained from the companion specimens.

B. Fatigue Properties of Metals

Until the last decade the only fatigue property of metals determined by testing and reported in handbooks and literature was the so-called "endurance limit" or fatigue limit. This was the stress amplitude in a completely reversed test (usually rotating bending) which was considered to be safe--that is, below this stress amplitude the fatigue life was considered to be infinite. The pioneering work of Coffin and Manson in 1954, where the cyclic plastic strain and fatigue life were shown to be related by a simple power function, led to a more detailed formulation of fatigue properties with metals over the entire life range from only a half cycle or a tension test to millions of cycles. The form of the Coffin-Manson relation is as follows:

$$\frac{\Delta\epsilon_p}{2} = \epsilon'_f (2N_f)^c \quad (2)$$

The plastic strain amplitude, $\Delta\epsilon_p/2$, is related to the life, $2N_f$, according to this equation in a log-log linear fashion, as shown in Fig. 6. The symbol $2N_f$ is used to indicate reversals or half cycles, while N_f means number of cycles to failure.* For a constant amplitude test, the number of reversals is equal to twice the number of cycles. In a variable amplitude test it is not always a simple matter to identify a cycle. However, half cycles or reversals can always be evaluated as peak-valley or valley-peak excursions. Section II. C. will be devoted to the matter of counting cycles during variable loading histories.

The representation of fatigue life in terms of plastic strain, while attractive from a fundamental viewpoint because of the intimate cause and effect relation between the two, is difficult to apply to practical engineering problems. This is because the engineer and designer seldom know the amount of cyclic plastic strain

*Usually taken as the separation of the specimen into two pieces.

present at the critical location in a member or part. Rather, they are more apt to be able to measure or estimate the total cyclic strain by using strain gages or methods of applied mechanics.

While it is common practice to change the strain to an equivalent elastic stress by using Hooke's law, it is well to remember that a portion of the total strain is not elastic whenever a fatigue problem exists.

The obsession that engineers have the cyclic stress has been one of the major impediments to the acceptance and application of contemporary approaches to fatigue analysis. The endurance limit concept is ingrained in the thinking of many engineers, and the idea of the S-N curve to represent the finite life region is still used as a basis for cumulative damage analysis by many engineering groups. The S-N curve in the finite life region is often represented as a power function of stress in a form similar to Eq. 2. This formulation was first suggested by H. O. Basquin in 1910 and is of the following form:

$$\frac{\Delta\sigma}{2} = \sigma'_f (2N_f)^b \quad (3)$$

Here the σ represents true stress. This equation implies a log-log linear relationship between stress and life, as shown in Fig. 7. Note that the straight line continues to lower and lower stresses with longer and longer lives and that the "endurance limit" concept is not included in this equation.

This elimination of the "endurance limit" is appropriate for cumulative fatigue damage evaluation, since it is well known that large overstrains common in real life situations will cause the "knee" of the S-N curve to be eradicated. Cyclic stresses below the endurance limit will then produce finite fatigue lives.

In addition, many metals of engineering interest do not exhibit an "endurance limit" even in the absence of a periodic overstrain. In fact, principally ferrous-based

metals and some other BCC metals are the only ones capable of developing an "endurance limit." The effect of overstrain in eliminating the endurance limit is illustrated for several steels in Fig. 8.

Mean stress effects may be included in a variety of ways, as shown in Fig. 9. For the purpose of this formulation of fatigue properties of metals, it is convenient to incorporate mean stress effects as an equivalent change in static strength. This consists of changing the coefficient in Eq. 3 from σ'_f to $(\sigma'_f - \sigma_o)$. Equation 3 may then be modified as follows:

$$\frac{\Delta\sigma}{2} = (\sigma'_f - \sigma_o) (2N_f)^b \quad (4)$$

To obtain an expression relating total strain, mean stress and life, Eq. 4 is divided by the Young's modulus, E, to obtain the elastic strain and added to Eq. 2 for the plastic strain, as shown in Fig. 10.

$$\frac{\Delta\epsilon}{2} = \frac{\Delta\epsilon_e}{2} + \frac{\Delta\epsilon_p}{2} = \left(\frac{\sigma'_f - \sigma_o}{E} \right) (2N_f)^b + \epsilon'_f (2N_f)^c \quad (5)$$

The two exponents and the coefficients are regarded as fatigue properties of the metal, and they are designated as follows:

- b = Fatigue strength exponent
- c = Fatigue ductility exponent
- ϵ'_f = Fatigue ductility coefficient
- σ'_f = Fatigue strength coefficient

By manipulating Eq. 2 and 3 to eliminate life and carrying the result to the form of Eq. 1, it can be shown that the cyclic strain hardening exponent, n' , is determined by the fatigue strength and ductility exponents as follows:

$$n' = \frac{b}{c} \quad (6)$$

Similarly, it can also be shown that the cyclic strength coefficient can be determined from the fatigue properties as follows:

$$K' = \frac{\sigma_f'}{(\epsilon_f')^{n'}} \quad (7)$$

When fatigue data are available so that the fatigue properties can be determined, it is advisable to use Eqs. 6 and 7 to determine n' and K' rather than using approximate values from the incremental step test. If appropriate fatigue data are not available, the following approximate relationships are sometimes useful in estimating fatigue properties of ductile steels from tensile data.

$$\begin{aligned} \sigma_f' &\approx \sigma_f = \text{True fracture strength} \\ &\approx S_u + 50 \text{ ksi}; S_u = \text{Ultimate tensile strength} \\ b &\approx -\frac{1}{6} \log \left(\frac{2\sigma_f}{S_u} \right) \\ &\approx -0.1 \text{ for soft steels} \\ &\approx -0.05 \text{ for hardest steels} \\ \epsilon_f' &\approx \epsilon_f = \text{True fracture ductility} \\ \epsilon_f &= \ln \left(\frac{100}{100 - \%RA} \right); \%RA = \text{Percent reduction in area} \\ &\approx -0.5 \text{ for soft steels to } -0.7 \text{ for hardened steels} \end{aligned}$$

The above crude approximations of the fatigue properties of steels should be used only for preliminary design estimates when proper laboratory data are not yet available.

C. Cycle Counting

Some of the cycle counting methods in use today for fatigue analysis are peak, level crossing, range, range-mean, range-pair, and rainflow. Of these various methods, rainflow or its equivalent range-pair has been shown to yield superior fatigue life estimates (2).

Recall that fatigue properties are determined from a constant amplitude testing. An irregular load history must be reduced into a series of constant amplitude events for comparison with the smooth specimen data. The concept of a cycle in an irregular history is difficult to define; however, a reversal can easily be defined as a change in sign in the loading. A constant amplitude sinusoidal cycle would contain two reversals. The apparent reason for the superiority of rainflow counting is that it combines load reversals in a manner that defines a cycle as a closed hysteresis loop. Each closed hysteresis loop has a strain range and mean stress associated with it that can be compared with the constant amplitude fatigue data in order to calculate fatigue damage.

In order to illustrate rainflow counting, consider the simple spectrum and the corresponding stress-strain response, shown in Fig. 11. The four events in the stress-strain response that resemble constant amplitude cycles are easily identified as a-d-a, c-b-c, d-e-d, and f-g-f. Rainflow counting recognizes these events as closed hysteresis loops and counts them as cycles. In this procedure the small event b-c is treated as an interruption of the overall event a-d. Although the events c-d and e-d appear identical in the strain time history, and would be counted as equally damaging by the range or range-mean method, the mean stresses and plastic strains are quite different even though the mean strain and strain ranges are equal. It should also be noted that mean stresses cannot be calculated directly from mean strains. The basic idea behind rainflow counting is to treat small events as interruptions of larger overall events and, in the simplest terms, to match the highest peak and deepest valley, then the next largest and smallest together, etc., until peaks and valleys have been paired.

III. METHODS OF FATIGUE DAMAGE ANALYSIS

A. Simulation of Stress-Strain Response

The purpose of simulating the stress-strain response is to determine the parameters necessary for cumulative damage fatigue analysis. Information such as stress amplitude, mean stress, elastic and plastic strain can be determined for each reversal in the load history. The most important feature of the model is its ability to correctly describe the history dependence of cyclic deformation. This so-called memory effect can best be illustrated in the stress-strain response, shown in Fig. 11. As the material deforms from a to b, it follows a path described by the cyclic stress-strain curve (Eq. 1) magnified by a factor of two, because it is a hysteresis loop rather than a monotonic loading. At point b the load is reversed and the material elastically unloads to point c. When the load is reapplied from c to d, the material elastically deforms to point b where the material remembers its prior history (i. e. from a to b) and deformation continues along path a to d as if event b-c never occurred.

To be exact the model should also have the capability of including the effects of cyclic hardening or softening and of cycle-dependent relaxation of mean stress, as shown in Fig. 12. In analyzing real structures, transient behavior is usually ignored and stable cyclic materials properties are used, thus eliminating the need to model cyclic hardening or softening. In a stationary random load history, cycle-dependent mean stress relaxation can usually be ignored, because it contributes little to the total fatigue damage. This is not meant to imply that mean stresses can be ignored. In certain types of block loading, particularly those with occasional large shifts in the mean, the presence of mean stresses and their relaxation may have a significant influence and should be included.

Martin (3) developed a computer model for cyclic deformation, based on a series of springs and frictional sliders, which is used to describe the hysteresis and cyclic memory effects exhibited by metals. This type of model requires a great deal of computation because of the number of equations involved. Wetzel (4) developed a similar model, based on an "availability concept," which reduces the computational aspects of the analysis and, as such, is much easier to program for a digital computer.

The cyclic stress-strain curve (Eq. 1) is approximated by a series of straight line segments or elements. The number and size of the elements is arbitrary, depending on the manner in which elements are used. A large number of elements (50-100) can be used where each element is used to its fullest extent. When a smaller number of elements is used, they are usually interpolated to obtain midrange values. The following rules govern the manner in which elements are used:

- (1) Start with the first element
- (2) Use them in order
- (3) Skip those elements unavailable for deformation
- (4) Continue until the control condition is reached.

For the purpose of illustration, a model consisting of ten elements will be used to simulate the stress-strain response of the spectrum shown in Fig. 11.

First, the largest strain (maximum or minimum) in the history must be determined. This point will lie on the cyclic stress-strain curve and serve as a reference for determining the stress associated with each reversal. The spectrum is arranged in such a manner that the largest strain is the first and last value in the history.

The stress-strain elements are then formed using Eq. 1, as illustrated in Fig. 13. Starting at point a, corresponding to a strain of -0.015 and a stress of -70 ksi, as determined from the cyclic stress-strain curve, the stress and strain elements are doubled, so that the cyclic loading curve is similar to the initial loading

curve but magnified by a factor of two. The availability coefficient of all the elements is set to -1, because the maximum strain was compressive. An availability of -1 means that all elements with an availability of -1 are available for tensile deformation but not compressive. Similarly, all elements with an availability of +1 are available for compressive deformation but not tensile. Once an element has been used for deformation, its availability is changed to the opposite sign. Simply stated this means that after an element is used in tension it must be used in compression before it can be used again in tension.

In traversing from a to b, six and one-half elements would be required but, since elements can only be used to the fullest extent, seven full elements are used. The stress and strain are incremented by seven elements with the resulting stress of 62 ksi and strain of 0.006 at b. The error between the calculated and observed strain is, of course, reduced when a greater number of line segments are used to describe the cyclic stress-strain curves. Since the first seven elements were used in tension, their availability sign is changed to +1, as shown in Fig. 14. One element is required to go from b to c. The availability is changed to -1, because the elements were used in compression. The stress and strain are also incremented by one element with the result of 2 ksi and 0.003, respectively.

Four elements are required to go from c to d. The availability matrix shows that elements 2 through 7 are unavailable for tensile deformation. Therefore, elements 1, 8, 9 and 10 must be used to makeup the four elements required to reach a strain of 0.015. The strain is incremented by 0.012, the stress by 68 ksi, the sum of elements 1, 8, 9 and 10. At this point all elements are available for compressive deformation. Reversal d-c requires four elements in compression with the resulting strain and stress of 0.003 and -46 ksi. The availability sign on the first four elements is changed to -1, indicating that they are available for tensile deformation for reversal e-d, which uses four elements in tension. All of the elements

are once again available for compressive deformation. The last three reversals are treated in the same manner as the first three except that the loading direction is changed, i. e. a-b is tensile, while d-f is compressive. The completed element matrix, Fig. 14, shows all of the elements that were used for each reversal.

Figure 15 shows the simulated stress-strain response for the spectrum, which is in excellent agreement with the measured response of Fig. 11.

Besides simulating the stress-strain response of the material, the model provides a convenient and efficient method of cycle counting. There are four closed hysteresis loops in this spectrum: a-d-a, b-c-b, d-e-d and f-g-f. A close examination of the element matrix will show that when a hysteresis loop is closed, one or more elements has been skipped.

For example, in reversal c-d, elements 3 through 8 were skipped indicating that a closed hysteresis loop consisting of elements 1 and 2 was formed. Similarly, in reversal e-d, elements 5 through 10 would be skipped if they were required, indicating a closed hysteresis loop of elements 1 through 4 was formed. The key to cycle counting is that a closed hysteresis loop is formed whenever the next element in the availability matrix is unavailable for deformation. Also, there are no skipped elements in a hysteresis loop, which means that every time element 5 was skipped a loop consisting of elements 1 through 4 was formed.

Once the cycles have been defined and the stress-strain response determined, the appropriate fatigue parameters can be determined, so that a damage analysis can be performed. Also, it should be noted that a cycle counting algorithm, completely independent of the material response model, can be developed along the lines of an availability concept as suggested by Richards, et al. (5).

B. Component Calibration Techniques

In many practical problems engineers and designers are required to evaluate the fatigue resistance of new components while they are at the drawing board or

prototype stage of development. One method for performing this type of analysis is the so-called "component calibration" technique, described by Landgraf (6), which requires a relationship between applied load and local strains, such as the one shown in Fig. 16. This type of information can be obtained analytically with a finite element model or experimentally by testing the component. The component would normally be tested by attaching strain gages to the critical locations and applying one load and unload cycle while measuring the load-strain response. However, this type of test will produce inaccurate data because of the cyclic hardening or softening characteristics of the material. For this reason, an incremental step type of test should be used in obtaining load-strain curves from a single component. Similarly, cyclically stable material properties should be used in any analytical calculations.

The conversion of applied load into strain is accomplished in exactly the same manner as strain was converted into stress. The load-strain response has all of the features normally associated with stress-strain response, i.e. hysteresis effects, memory, and cyclic hardening and softening. The transient response is normally neglected, so that the load-strain response model only accounts for hysteresis and memory effects. From a computational viewpoint, this technique is exactly the same as those described in the last section for stress-strain response. In fact, the load-strain and stress-strain response models can be combined, so that the applied load can be converted to both the local stress and strain with one simple computer algorithm.

C. Notch Analysis

1. Neuber's Rule

In dealing with real components, it is often necessary to relate the nominal loads or strains to the maximum stresses and strains at the critical location. Neuber derived a rule which applies when the material at the notch root deforms nonlinearly. The theoretical stress concentration, K_t , is equal to the geometric mean of the actual stress and strain concentration factors, K_ϵ and K_σ .

$$K_t = (K_\sigma K_\epsilon)^{\frac{1}{2}} \quad (8)$$

Topper, et al. (7) modified Neuber's rule for use in cyclic loading applications by substituting the fatigue notch factor, K_f , for the stress concentration factor and rewriting Eq. 8 in the following form:

$$K_\sigma = \frac{\Delta\sigma}{\Delta S}$$
$$K_\epsilon = \frac{\Delta\epsilon}{\Delta e} \quad (9)$$
$$K_f = \left(\frac{\Delta\sigma}{\Delta S} \frac{\Delta\epsilon}{\Delta e} \right)^{\frac{1}{2}}$$

where

$\Delta\sigma$ = Stress range at notch root

ΔS = Nominal stress range

$\Delta\epsilon$ = Strain range at notch root

Δe = Nominal strain range

This relationship is conveniently used in the following form:

$$K_f^2 \Delta S \Delta e = \Delta\sigma \Delta\epsilon \quad (10)$$

All terms on the left side are determinable for each reversal from the load history and cyclic stress-strain response of the material, and those terms on the right side represent the local stress-strain behavior of the material at the notch root. The terms on the left side are a determinable constant for each reversal and the result is an equation of the form, $xy = c$, which is a rectangular hyperbola. When the nominal strains are elastic, Eq. 10 may be used in the following form:

$$\Delta\sigma \Delta\epsilon = \frac{(K_f \Delta S)^2}{E} \quad (11)$$

Combining this form with Eq. 1, an expression for the notch stress becomes

$$\frac{\Delta\sigma^2}{E} + \Delta\sigma \left(\frac{\Delta\sigma}{K_f} \right)^{1/n'} = \frac{(K_f \Delta S)^2}{E} \quad (12)$$

This equation is easily solved using the Newton-Raphson iteration technique. Once the notch stress is obtained, it can be used in Eq. 1 to solve for the elastic and plastic strains at the notch root. After each reversal, a new axis is defined and the right-hand side of Eq. 12 recalculated in order to solve for the new stress and strain range. This process is illustrated in Fig. 17.

One of the difficulties in applying this type of analysis is the constant accrual of error in the stress and strain, because each point is referenced to the end of the previous reversal rather than the original starting stress and strain. One method employed to overcome numerical difficulties is to use a straight line approximation developed by Stadnick (8), as shown in Fig. 18. The slope, m , of the line is given by

$$m = \frac{K_f S_{\max} - \sigma_{\max}}{K_f \frac{S_{\max}}{E} - \epsilon_{\max}} \quad (13)$$

and the stresses calculated from

$$S = \frac{\sigma - m\epsilon}{K_f \left(1 - \frac{m}{E} \right)} \quad (14)$$

While this approach is not exact, it has the advantage of referencing all deformations to the original stresses and strains. This results in less total error than a Neuber analysis that defines a new origin at each reversal.

An alternate approach is to directly incorporate Neuber's rule into the material response model. There is a one-to-one correspondence between nominal and notched closed hysteresis loops, i.e. for each closed hysteresis loop of amplitude, ΔS and $\Delta\epsilon$, there is a closed hysteresis loop of amplitude, $\Delta\sigma$ and $\Delta\epsilon$, at the notch root. The elements, ΔS and $\Delta\epsilon$, have already been determined for the stress-strain response

model. Notch stress-strain elements, $\Delta\sigma$ and $\Delta\epsilon$, are then determined for each nominal stress-strain element using a combination of Eqs. 1 and 10. The new notch elements are then used in exactly the same manner as the original stress-strain elements described in Section III. A. Whenever an element is used in the nominal stress-strain behavior, it is also used in the notch stress and strain response; conversely, whenever an element is skipped in the nominal behavior, it is also skipped in the notch response. The significance of this is that, once the nominal stress-strain response is obtained, the notch response is automatically determined. For example in Fig. 15, reversal c-d uses elements 1, 8, 9 and 10 to obtain the nominal stress-strain response. Notch elements 1, 8, 9 and 10 would be used to obtain the notch response. Material response, cycle counting, component calibration and notch response can be combined into a single model for efficient computation of fatigue damage similar to that of Socie (9).

2. Fatigue Notch Factor

The fatigue notch factor, K_f , is always less than or equal to the theoretical stress concentration factor, K_t , and its determination is an important part of the notch analysis. The appropriate value of K_f depends not only on the geometry but also on the material, thickness, surface finish, and stress gradient. For notched parts, the appropriate value of K_f can be estimated from Peterson's equation

$$K_f = 1 + \frac{K_t - 1}{1 + \frac{a}{r}} \quad (15)$$

where r = Notch root radius

a = Material constant, depending on strength and ductility

For heat treated steels the following equation may be used to estimate a

$$a \text{ (in.)} = 10^{-3} \left(\frac{300}{S_u} \right)^{1.8} \quad (16)$$

where S_u = Ultimate tensile strength, ksi

Experimentally, K_f can be determined for any component by performing fatigue tests and plotting the product, $\Delta\sigma \Delta\epsilon$, for the smooth specimen and, $\Delta S \Delta\epsilon$, for the component, as will be discussed later in connection with Fig. 31. The fatigue notch factor is the difference between the two curves shown in the figure.

D. Cumulative Damage Analysis

Cumulative damage fatigue analysis is usually based on the Palmgren-Miner linear damage rule. Fatigue damage is computed by linearly summing cycle ratios for the applied loading history, as indicated in the following equation.

$$\text{Damage} = \sum \frac{n_i}{N_{fi}} \quad (17)$$

where: n_i = Observed cycles at amplitude, i
 N_{fi} = Fatigue life at constant amplitude, i

After the fatigue damage for a representative segment or block of load history has been determined, the fatigue life in blocks is calculated by taking the reciprocal. Other more complex procedures for summing damage such as the double linear damage concept and Corten-Dolan approach are not necessary for accurate life predictions for irregular loading provided the local σ - ϵ at the point of crack initiation is known. Special applications such as high temperature fatigue, where there is an interaction between creep and fatigue may require additional complications in the damage summation portion of the analysis.

The fatigue life for any cycle or reversal can be determined from Eq. 5.

$$\frac{\Delta\epsilon}{2} = \left(\frac{\sigma'_f - \sigma_0}{E} \right) (2N_f)^b + \epsilon'_f (2N_f)^c \quad (5)$$

The mean stress, σ_0 , and cyclic strain range, $\Delta\epsilon$, has been determined from the material response model, and the four fatigue properties have been determined from constant amplitude life tests. Equation 5 cannot be explicitly solved for life because of the negative fractional exponents involved, but can easily be solved using Newton-Raphson or interval halving iteration techniques. The main advantage of this formulation of fatigue damage is that it eliminates the need to determine elastic and plastic components of the total strain. In other formulations of fatigue damage, the relative amounts of elastic and plastic strain are dependent on the choice of the cyclic stress-strain properties, where a small difference can produce a large difference in life estimates, especially at low strain amplitudes and long lives. Also, mean stress has a greater effect at longer lives because the elastic term dominates, which is in agreement with observed behavior.

IV. APPLICATION OF A STRAIN BASED ANALYSIS TO THE SAE CUMULATIVE FATIGUE DAMAGE TEST PROGRAM

A. Review of Test Program

The test program (10) will be briefly reviewed for those readers unfamiliar with it. Three load histories, Fig. 19, were selected from magnetic tape recordings of nominal strain from actual components under operating conditions. These load histories were designated (a) suspension with a dominant compressive mean, (b) transmission which has a tensile mean, and (c) bracket which is a random narrow band vibration. The analog signals were digitalized and filtered to provide a sequence of peaks and valleys that were normalized, so that the largest value in the spectrum was set equal to 1999. No attempt was made to preserve the frequency content of these data.

The specimen, Fig. 20, provided both axial and bending stresses and strains at the notch root, which is typical of many production components. Loads were applied to the specimen (component) through a monoball fixture, that allowed both tensile and compressive loads to be applied. Variable amplitude tests consisting of 57 specimens were performed, using the three load histories scaled to different maximum loads to produce fatigue lives ranging from 10^4 to 10^8 reversals, as shown in Table I. Also, constant amplitude fully reversed data were obtained for this specimen.

Two commonly used structural steels, U. S. Steel's Man-Ten and Bethlehem's RQC-100, were used in this program. Mechanical properties of these steels are shown in Table II. Both, the monotonic and cyclic stress-strain curves for these materials are shown in Figs. 21 and 22. The strain-life curves are shown in Figs. 23 and 24. It should be noted that there is plastic deformation in Man-Ten at 10^6 reversals, which is normally thought to be in the elastic range.

B. Nominal Strain-Life Analysis

A nominal strain-life analysis will be used to predict the crack initiation life of the specimen, shown in Fig. 20. The following steps are required for performing the analysis using smooth specimen material properties.

a. Material Properties

Material properties required for this analysis have been determined from a series of fatigue tests and are listed in Table II. Specifically, the required fatigue properties are: fatigue strength coefficient and exponent, fatigue ductility coefficient and exponent, and the elastic modulus. If the material properties were unknown, they would have to be determined by a series of smooth specimen fatigue tests or estimated from tensile data. A discussion of this procedure can be found in Section II. B.

b. Theoretical Stress/Strain Concentration Factor

The elastic stress concentration factor for the circular notch was estimated to be 3.0. Actual strain gage measurements at the notch root show the strain concentration factor to be approximately 2.93 when the reduced section of the specimen is treated as a simple beam. In actual practice the stress concentration factor can be determined from stress concentration tables (11), finite element analysis, or from experimental stress analysis methods applied to actual components.

c. Nominal Strain History

A difficult and expensive part of the analysis is to obtain the field loading for a component. The loads are usually recorded on magnetic tape, and then must be filtered and digitalized to obtain a sequence of peaks and valleys. A digitized sequence of load peaks and valleys were obtained from the SAE Fatigue Design and Evaluation Committee and are listed in Ref. (10). Loads were converted to nominal strains by assuming that the reduced section of the specimen acts as a simple beam subjected to axial and bending stresses.

The following relationship from elementary beam theory was used.

$$e = \frac{Mc}{IE} + \frac{P}{AE} \quad (18)$$

for the keyhole specimen:

$$e = 7.26 \frac{P}{E}$$

where: e = Nominal strain
 P = Applied load, kips
 E = Elastic modulus, ksi

Of course, if nominal strains were available, this conversion would be unnecessary.

d. Convert Nominal Strains to Notch Strains

The nominal strains are converted to notch strains through the simple relationship:

$$\epsilon = K_t e \quad (19)$$

for the keyhole specimen:

$$\epsilon = 3.0 e$$
$$\epsilon = \frac{21.8 P}{E}$$

This type of conversion, as well as the load-strain conversion, assumes elastic behavior both nominally and at the notch root.

e. Rainflow Count Notch Strains

Computational aspects of rainflow counting are described in Appendix A and will not be elaborated upon here.

f. Calculate and Sum Fatigue Damage

Fatigue damage can be calculated during the rainflow counting procedure on a cycle-by-cycle basis or from a histogram of rainflow counted ranges. The fatigue damage for each cycle is calculated from Eq. 17. Equation 5, with the mean stress set equal to zero, is used to calculate the fatigue life of each range.

The results of the nominal strain-life analysis are shown both in Table III and Fig. 25. The computer algorithm used for these predictions is listed in Appendix A. In this approach the effect of mean stress is not included. By assuming elastic behavior, the mean stress could be calculated from mean strain; however, this could lead to considerable errors, as was shown in Fig. 11. Sequence effects are included only in the rainflow counting procedure.

An alternate approach to the above analysis would be to determine the nominal strain-life curve for the individual component through a series of constant amplitude fatigue tests. Then this strain-life curve would be used in place of the actual material properties, and the notch strains need not be determined. This type of approach is particularly useful in evaluating welded structures, where the stress concentration factors and mean stresses are difficult to obtain.

C. Component Calibration Analysis

1. Experimental Determination of Load-Strain Curve

Component calibration is the name given to the method where applied loads are converted to notch root strains retaining all sequence effects. This method is applicable for both elastic and plastic strains and requires a relationship between applied load and notch root strain. A strain gage was mounted in the notch root, and the relationship between applied load and notch root strain was obtained from a monotonic tension test of specimens/components made from Man-Ten and RQC-100. Then the specimen was subjected to an incremental step type of test in order to cyclically stabilize the material. Monotonic and cyclic load-strain curves are shown in Figs. 26 and 27 for Man-Ten and RQC-100, respectively. The same type of cyclic behavior is noted in both the smooth specimen and component, i.e. cyclic hardening for Man-Ten and cyclic softening for RQC-100. Cyclic plasticity and, hence, fatigue damage in the cyclically stable component is considerably different from that calculated using the monotonic load-strain response. For this reason, only cyclically stable load-strain curves should be used in the analysis.

2. Finite Element Determination of Load-Strain Curve

The specimen was a finite element modeled with the grid pattern shown in Fig. 28. A program developed at the University of Illinois for the cyclic plastic

analysis of notched plates, was used to generate the load-strain curves shown in Fig. 16. This program uses constant strain triangular elements with kinematic hardening. A piecewise linear solution is obtained for each load increment. Cyclically stable properties for the cyclic strength coefficient and strain hardening exponent were used in the analysis. The correlation between the experimental finite element analysis is quite good.

3. Load-Strain Conversion and Fatigue Analysis

An advantage of the component calibration techniques is that it accounts for notch root plasticity, and it does not require the determination of the stress concentration factor. The method, outlined below, does not include mean stress. The effect of mean stress is discussed in the next section.

a. Material Properties

Same as those used in nominal strain-life analysis.

b. Load-Strain Curve

An equation of the form of Eq. 1 was fit to the load-strain curves in Figs. 26 and 27

$$e = \frac{P}{C_1} + \left(\frac{P}{C_2} \right)^{1/D} \quad (20)$$

with the following results (6):

	<u>Man-Ten</u>	<u>RQC-100</u>
C_1	1.41×10^6	1.41×10^6
C_2	6.67×10^4	6.55×10^4
D	0.39	0.31

c. Load History

Same as nominal strain analysis.

d. Rainflow Count Load History

Rainflow counting is used to obtain the load ranges for conversion to notch root strains.

e. Convert Load Ranges to Strain Amplitude

Divide each load range by two to obtain load amplitude. For each load amplitude, identified by rainflow counting, enter the load-strain curve to obtain notch root strain amplitude. This strain amplitude is then used to calculate fatigue damage.

f. Calculate and Sum Fatigue Damage

Same as nominal strain-life analysis.

Results of this analysis are shown in Table III and Fig. 29. Correlation between predicted lives and test data is somewhat better than the nominal strain-life analysis primarily because notch root plasticity is accounted for. The only difference between the two analyses is the manner in which notch root strains are obtained from applied loads. The computer algorithm used for this analysis is found in Appendix B.

4. Load-Stress-Strain Conversion and Fatigue Analysis

The analysis, outlined below, is a refinement of the previous one by accounting for the mean stress of each load reversal. The stress-strain response of each reversal must be determined on a reversal-by-reversal basis retaining all sequence effects. A detailed description of this procedure may be found in Refs. (9).

a. Material Properties

In addition to the fatigue properties previously used, the cyclic stress-strain response of the material must be known. The cyclic strength coefficient and strain hardening exponent may be determined from the fatigue properties using Eqs. 6 and 7.

b. Load-Strain Curve

Determined by methods used in Sections I and II.

c. Load History

Same as nominal strain analysis.

d. Material Response Model

A model for following the load-strain and stress-strain response must be programmed for a digital computer using the concepts discussed in previous sections.

- e. Follow the Load-Stress-Strain Response of the Specimen on a Reversal-by-Reversal Basis

The strain range and mean stress of each reversal in the load history is obtained from the material stress-strain response model. The mechanics of the computer algorithm used for these calculations are discussed in Appendix C.

- f. Rainflow Count Applied Loads or Notch Root Strains

The simplest method of rainflow counting is to use the material response model, as illustrated in Appendix C.

- g. Calculate and Sum Fatigue Damage

Fatigue damage is calculated for each closed hysteresis loop identified by rainflow counting. Equation 5 is solved for fatigue life and damage calculated from Eq. 17.

The results of this analysis are shown in Fig. 30 and Table III. The only difference between this analysis and the previous one is the inclusion of mean stress effects. Computational aspects of the analysis are increased because of the material response model calculations. However, once the procedure is programmed for a digital computer, the analysis can easily be performed. Fairly accurate life predictions can be obtained when notch root plasticity and mean stress effects are properly accounted for.

D. Notch Analysis

1. Experimental Determination of the Fatigue Notch Factor

The fatigue notch factor was experimentally determined from a series of constant amplitude fully reversed fatigue tests of the specimen. A Neuber curve for the smooth specimen properties of Man-Ten and RQC-100 was constructed by plotting the product of stress and strain range versus fatigue life, as shown in Figs. 31 and 32. These curves are obtained from the cyclic stress-strain and strain-life curves for each material.

Nominal stresses were obtained from the applied loads using the equation developed in Section IV. B.

$$e = 7.26 \frac{P}{E} \quad (18)$$

$$S = 7.26 P$$

Since the nominal stresses are assumed to be elastic, the Neuber parameter reduces to

$$\frac{\Delta S^2}{E}$$

and is plotted on the same curve as the smooth specimen data. The fatigue notch factor is then the square root of the difference between the two curves and is equal to 2.6 for this specimen configuration. This method requires several component fatigue tests and, in general, would not be applicable to prototype work.

2. Analytical Determination of the Fatigue Notch Factor

The theoretical stress concentration factor was estimated to be that of a circular hole in a semi-infinite plate for which $K_t = 3.0$. Finite element analysis used to develop the load-strain curve shows that K_t should be 3.08 and, experimentally, strain gage measurements show it to be 2.93. The fatigue notch factor is then calculated from Peterson's equation

$$K_f = 1 + \frac{K_t - 1}{1 + \frac{a}{r}} \quad (15)$$

for the keyhole specimen

$$a = \begin{array}{l} 0.01 \text{ for Man-Ten} \\ 0.004 \text{ for RQC-100} \end{array}$$

$$r = 0.1875 \text{ in.}$$

$$K_f = \begin{array}{l} 2.90 \text{ for Man-Ten} \\ 2.96 \text{ for RQC-100} \end{array}$$

3. Neuber Notch Analysis

Neuber notch analysis is most often used when the service history is in the form of nominal strains. The analysis for the keyhole specimen proceeds as follows:

a. Material Properties

Same as load-stress-strain analysis.

b. Load History

Applied loads were converted to nominal stresses from Eq. 19.

c. Fatigue Notch Factor

Determined by methods of Sections I and II.

d. Material Response Model

A model for following the stress-strain response of the notch root and Neuber's rule must be programmed for a digital computer.

e. Rainflow Count Stress

The stress history is rainflow counted to obtain nominal stress hysteresis loops (stress ranges). Mean stress at the notch root is obtained from the material response model.

f. Determine Notch Root Stresses and Strains on a Reversal-by-Reversal Basis

Equation 12 is solved for each hysteresis loop to obtain notch root stress amplitude. This stress is then used to obtain strain amplitude for damage calculations.

g. Calculate and Sum Fatigue Damage

Same as load-stress-strain analysis.

The results of this analysis for a fatigue notch factor equal to 2.6 is shown in Fig. 33 and Table III. The computational aspects are discussed in detail in Appendix D, which also contains a computer listing.

V. DISCUSSION OF LIMITATIONS OF APPROACH

The reader is reminded that the analysis described above is limited to predicting the fatigue crack initiation life of members subjected to variable loading histories. Analogous techniques for estimating the rate at which fatigue cracks will grow in service are not yet well developed. Fatigue crack propagation under variable loading history is the subject of current research. In this connection it is important to utilize non-arbitrary definition for fatigue crack initiation. In the work described in this paper, it has been assumed that a crack of engineering significance will form at the most highly strained region at the same time as a smooth specimen subjected to the same stress-strain history would fracture into two pieces. While this is satisfactory for engineering estimates, no quantitative definition of the size of an initiated crack has been given although current research is being done in this area. Both crack initiation life and crack propagation life must be estimated in order to optimize the material and geometry for the application at hand. This is important to the efficient design for routine applications and essential for the design of advanced machine.

Also, note that a uniaxial state of stress has been assumed to exist in the most highly strained region, so that life can be estimated on the basis of smooth specimen data obtained by uniaxial testing. This assumption is reasonably valid for a number of engineering structural elements, but is not generally true. For example, if thick sections are involved, biaxial stresses will be present at notch roots which, in general, will constrain plastic deformation, so that less fatigue damage will occur than predicted using uniaxial assumptions. Thus life predictions, using the methods described herein, will tend to be conservative. A first-order correction for biaxial stresses and strains might be to use an equivalent strain calculated in a manner similar to that used for yielding.

Then methods suggested here work best for reasonably ductile, homogeneous, isotropic materials. Applications of these methods in the case of metals with controlling internal discontinuities, such as present in cast metals or high hardness steels with non-metallic inclusions, requires that one treat the cast material as micro-notched metal, as described by Mitchell (12). A similar approach can be employed on weldments as suggested by Lawrence and his coworkers (13). The weldment problem is further complicated by the presence of three distinct zones of metal, i.e. base metal, weld metal, and the heat effected zone. In this case it may be necessary to characterize the mechanical resistance of the separate zones. A similar difficulty arises in applying these techniques to case hardened parts.

Other factors that have been ignored in the analysis include the influence of the environment, temperature, frequency, hold times, wave-shape effects, dynamic strain aging, etc. These factors are particularly crucial when the member is subjected to elevated temperature during operation and when the design life is long. For long lives, where the designed stresses are kept low enough to avoid significant cyclic plasticity even at the notch root, factors such as the initial residual stresses and assembly stresses are of prime importance in determining fatigue performance. Effects of design and fabrication details are much more important in determining the fatigue performance than are the bulk properties of the metal. Thus, the predictive techniques described here are more appropriate for applications to low cycle fatigue problems (i.e. $< 10^6$ cycles) where significant cyclic plasticity occurs, at least occasionally, in the most highly strained region.

In a more optimistic vein, the approach suggested here can be a powerful tool for reaching engineering decisions concerning the low cycle fatigue crack initiation life of members subjected to virtually any history of loading. Of prime importance is the utilization of a correct cycle counting procedure that identifies close hysteresis loops, so that the damage done can be related to constant amplitude baseline data.

Even the crude approaches, wherein the S-N curve of a component (e. g. weld joint) is used in conjunction with linear damage summation methods, are reasonably accurate provided the correct cycle counting method is used.

A knowledge of proper methods for cycle counting also permits the test engineer to edit service load spectra, so that laboratory test time can be greatly reduced without significantly altering the basic damage content of the spectrum. The spectrum editing approach is superior to the technique of increasing maximum operating load levels in order to shorten the test time, because such large loads may eliminate or induce residual stresses in the highly strained region that can have a large influence on the fatigue life of the member.

In this connection the approach is also useful for performing "sensitivity studies," as illustrated by Socie (9). One can quickly evaluate the relative merits of one material versus another for a given part geometry subjected to the same load history. Likewise, the influence of minor modification in the part geometry on its fatigue performance may be quickly evaluated. Finally, the relative fatigue lives of two parts made of a particular metal subjected to different load histories can be evaluated.

APPENDIX A

Computer Program for Nominal Strain-Life Analysis and Rainflow Counting

The following computer program was used to make the fatigue life predictions based on a nominal strain-life approach.

Input Variables

EF	Fatigue Ductility Coefficient
C	Fatigue Ductility Exponent
SF	Fatigue Strength Coefficient
B	Fatigue Strength Exponent
E	Elastic Modulus
SCALE	Scale Factor
AKT	Fatigue Notch Factor
NPEAKS	Number of Data Points
DATA	Sequence of Peaks and Valleys

Major Calculation Variables

AV	Availability Matrix
RANGE	Maximum Range of Data
SEG	Segment or Element Size for Rainflow Counting
RUN	Running Total of Input Data
SGN	+ 1 if Tensile Load; -1 if Compressive Load
DAMAGE	Fatigue Damage
STRAIN	Strain Amplitude
EST	Cycles to Failure for Strain Range

The overall flow diagram for all of the programs is shown in Fig. A1 with a detailed flow diagram for this analysis shown in Fig. A2. If a histogram of rainflow counted ranges is desired, the following statement is added to the fatigue damage calculation: $HIST(J) = HIST(J) + 1$. Of course, the dimension statement must be changed and the array initialized.

```
DIMENSION DATA(6000),AV(51)
TYPE 9
90 FORMAT (' EF,C,SE,E,E')
ACCEPT 100,EF,C,SE,B,E
100 FORMAT (5E)
TYPE 91
91 FORMAT (' SCALE,KT')
ACCEPT 101,SCALE,AKT
101 FORMAT (2F)
CALL IFILE(1,'BRACK')
READ(1,102)NPEAKS
102 FORMAT (6X,15)
READ(1,103)(DATA(I),I=1,NPEAKS)
103 FORMAT (6X,14F5.0)
MAX=1
MIN=1
DO 200 I=1,NPEAKS
IF (DATA(I).GT.DATA(MAX)) MAX=I
IF (DATA(I).LT.DATA(MIN)) MIN=I
200 CONTINUE
DO 201 I=1,NPEAKS
DATA(I)=DATA(I)*SCALE/999.*AKT*7.26/E
201 CONTINUE
RANGE=DATA(MAX)-DATA(MIN)
SEG=RANGE/50.
ISTART=MAX
IF (ABS(DATA(MIN)).GT.ABS(DATA(MAX))) ISTART=MIN
RUN=DATA(ISTART)
SGN=RUN/ABS(RUN)
DO 202 I=1,51
AV(I)=SGN
202 CONTINUE
ISTART=ISTART+1
IF (ISTART.GT.NPEAKS) ISTART=1
ISTOP=NPEAKS
DAMAGE=0.
300 DO 400 I=ISTART,ISTOP
J=0
SGN=1
IF (DATA(I).LT.RUN) SGN=-1.
301 J=J+1
RUN=RUN+SEG*SGN
AV(J)=SGN
IF (AV(J+1).NE.SGN) GO TO 350
STRAIN=FLCAT(J)*SEG/2.
EST=(STRAIN*E/SP)**(1./E)
302 Y1=STRAIN-E*EST**C-SP/E*EST**B
Y2=-C*EF*EST** (C-1.)-B*SP/E*EST** (E-1.)
EST=EST-Y1/Y2
IF (ABS(Y1).GT.0.01*STRAIN) GO TO 302
DAMAGE=DAMAGE+2./EST
303 J=J+1
IF (J.GE.51) GO TO 400
IF (AV(J+1).EQ.SGN) GO TO 303
350 IF ((DATA(I)-RUN)*SGN+0.01*SEG.GE.0.) GO TO 301
400 CONTINUE
IF (ISTART.EQ.1) GO TO 401
ISTOP=ISTART-1
ISTART=1
GO TO 300
401 DAMAGE=1./DAMAGE
TYPE 104,DAMAGE
104 FORMAT (' BLOCKS TO FAILURE ',E)
STOP
END
```

APPENDIX B

Computer Program for Load-Notch Strain Analysis

Only three lines of the preceding program are changed to use a load-strain curve in the analysis.

First, the constants describing the load-strain curve must be read into the program.

ACCEPT 100, SCALE, C1, C2, D

Second, the load is calculated from the segment number and the strain is then calculated from the load.

$$\text{ALOAD} = \text{J} * \text{SEG}/2$$

$$\text{STRAIN} = \text{ALOAD}/\text{C1} + (\text{ALOAD}/\text{C2}) ** 1/\text{D}$$

```
DIMENSION DATA(6000),AV(51)
TYPE 90
90  FORMAT(' EF,C,SF,E,E')
ACCEPT 100,EF,C,SF,B,E
100  FORMAT(5E)
TYPE 91
ACCEPT 100,SCALE,C1,C2,D
91  FORMAT(' SCALE,C1,C2,D')
CALL IFILF(1,'SUSP')
102  READ(1,102)NPEAKS
FORMAT(6X,5)
103  READ(1,103)(DATA(I),I=1,NPEAKS)
FORMAT(6X,14F5.0)
MAX=1
MIN=1
DO 200 I=1,NPEAKS
IF (DATA(I).GT.DATA(MAX)) MAX=I
IF (DATA(I).LT.DATA(MIN)) MIN=I
200  CONTINUE
DO 201 I=1,NPEAKS
DATA(I)=DATA(I)*SCALE/999.
201  CONTINUE
RANGE=DATA(MAX)-DATA(MIN)
SEG=RANGE/50.
ISTART=MAX
IF (ABS(DATA(MIN)).GT.ABS(DATA(MAX))) ISTART=MIN
RUN=DATA(ISTART)
SGN=RUN/ABS(RUN)
DO 202 I=1,51
202  AV(I)=SGN
CONTINUE
ISTART=ISTART+1
IF (ISTART.GT.NPEAKS) ISTART=1
ISTOP=NPEAKS
DAMAGE=0.
300  DO 400 I=ISTART,ISTOP
J=0
SGN=1
301  IF (DATA(I).LT.RUN) SGN=-1.
J=J+1
RUN=RUN+SEG*SGN
AV(J)=SGN
IF (AV(J+1).NE.SGN) GO TO 350
ALOAD=FLOAT(J)*SEG/2.
STRAIN=ALOAD/C1+(ALOAD/C2)**(1./D)
EST=(STRAIN*E/SF)**(1./B)
302  Y1=STRAIN-EF*EST**C-SF/E*EST**B
Y2=-C*EF*EST**C-1.-B*SF/E*EST**B-1.
EST=EST-Y1/Y2
IF (ABS(Y1).GT.0.01*STRAIN) GO TO 302
DAMAGE=DAMAGE+2./EST
303  J=J+1
IF (J.GE.51) GO TO 400
IF (AV(J+1).EQ.SGN) GO TO 303
350  IF ((DATA(I)-RUN)*SGN+0.01*SEG.GE.0.) GO TO 301
400  CONTINUE
IF (ISTART.EQ.1) GO TO 401
ISTOP=ISTART-1
ISTART=1
GO TO 300
401  DAMAGE=1./DAMAGE
TYPE 104,DAMAGE
104  FORMAT(' BLOCKS TO FAILURE ',E)
STOP
END
```

APPENDIX C

Computer Program for Load-Stress-Strain Analysis

The preceding program is modified to include mean stress effects by adding a section to calculate the stress that corresponds to each strain element. Three new variables are introduced:

STRESS	An Array Containing the Stress for Each Element
SM	Mean Stress
STRS	Mean Stress Reference

```

DIMENSION DATA(6000),AV(51),STRESS(52),STRAIN(51)
TYPE 90
FORMAT(' EF,C,SF,B,E')
ACCEPT 100,EF,C,SF,B,E
100 FORMAT(5E)
SHE=B/C
CSC=SF/EF**SHE
TYPE 91
ACCEPT 100,SCALE,C1,C2,D
FORMAT(' SCALE,C1,C2,D')
CALL IFILE(1,'BRACK')
102 READ(1,102)NPEAKS
FORMAT(6X,15)
103 READ(1,103)(DATA(I),I=1,NPEAKS)
FORMAT(6X,14F5.2)
MAX=1
MIN=1
DO 200 I=1,NPEAKS
IF (DATA(I).GT.DATA(MAX)) MAX=I
IF (DATA(I).LT.DATA(MIN)) MIN=I
200 CONTINUE
DO 201 I=1,NPEAKS
DATA(I)=DATA(I)*SCALE/999.
201 CONTINUE
RANGE=DATA(MAX)-DATA(MIN)
SEG=RANGE/50.
ISTART=MAX
IF (ABS(DATA(MIN)).GT.ABS(DATA(MAX))) ISTART=MIN
RUN=DATA(ISTART)
SGN=RUN/ABS(RUN)
DO 202 I=1,51
202 AV(I)=SGN
CONTINUE
DO 500 I=1,50
ALOAD=FLCAT(I)*SFG/2.
500 STRAIN(I)=ALOAD/C1+(ALOAD/C2)**(1./D)
CONTINUE
STRAIN(51)=ABS(RUN)/C1+(ABS(RUN)/C2)**(1./D)
DO 510 I=1,51
511 SIG=STRAIN(I)*E
Y1=STRAIN(I)-SIG/E-(SIG/CSC)**(1./SHE)
Y2=-1./E-(1./SHE)*(SIG/CSC)**(1./SHE-1.)/CSC
SIG=SIG-Y1/Y2
IF (ABS(Y1).GT.0.C1*STRAIN(I)) GO TO 511
510 STRESS(I+1)=SIG
CONTINUE
STRS(1)=0.
STRS=STRESS(52)*SGN
ISTART=ISTART+1
IF (ISTART.GT.NPEAKS) ISTART=1
ISTOP=NPEAKS
DAMAGE=0.
300 DO 400 I=ISTART,ISTOP
J=0
SGN=1
301 IF (DATA(I).LT.PUN) SGN=-1.
J=J+1
RUN=RUN+SFG*SGN
STRS=STRS+(STRESS(J+1)-STRESS(J))*SGN*2.
AV(J)=SGN
IF (AV(J+1).NE.SGN) GO TO 350
SM=STRS-SIFESS(J+1)*SGN
EST=(STRAIN(J)*E/(SF-SM))**(1./B)
302 Y1=STRAIN(J)-EF*EST**C-(SF-SM)/E*EST**B
Y2=-C*EF*EST**C-(1.-B)*(SF-SM)/E*EST**B
EST=EST-Y1/Y2
IF (ABS(Y1).GT.0.C1*STRAIN(J)) GO TO 302
DAMAGE=DAMAGE+2./EST
303 J=J+1
IF (J.GE.51) GO TO 400
IF (AV(J+1).EQ.SGN) GO TO 303
350 IF ((DATA(I)-RUN)*SGN+C.01*SEG.GE.0.) GO TO 301
400 CONTINUE
IF (ISTART.EQ.1) GO TO 401
ISTOP=ISTART-1
ISTART=1
GO TO 300
401 DAMAGE=1./DAMAGE
TYPE 104,LAMAGF
104 FORMAT(' BLOCKS TO FAILURE ',E)
STOP
END
```

APPENDIX D

Computer Program for Neuber Notch Analysis

The changes made to the nominal strain analysis program are the same as those made in the preceding section except the stresses are calculated using Neuber's rule.

```
/**
DIMENSION DATA(6000),AV(51),STRESS(52),STRAIN(51)
TYPE 90
90  FORMAT(' EF,C,SF,E,E')
ACCEPT 100,EF,C,SF,B,E
100  FORMAT(5E)
SHE=B/C
CSC=SF/EF**SHE
TYPE 91
ACCEPT 100,SCALE,AKF
91  FORMAT(' SCALE,KF')
CALL IFILE(1,'BRACK')
READ(1,102)NPEAKS
102  FORMAT(6X,I5)
READ(1,103)(DATA(I),I=1,NPEAKS)
103  FORMAT(6X,14F5.0)
MAX=1
MIN=1
DO 200 I=1,NPEAKS
IF(DATA(I).GT.DATA(MAX)) MAX=I
IF(DATA(I).LT.DATA(MIN)) MIN=I
200  CONTINUE
DO 201 I=1,NPEAKS
DATA(I)=DATA(I)*SCALE/999.*7.26
201  CONTINUE
RANGE=DATA(MAX)-DATA(MIN)
SEG=RANGE/50.
ISTART=MAX
IF(ABS(DATA(MIN)).GT.ABS(DATA(MAX))) ISTART=MIN
RUN=DATA(ISTART)
SGN=RUN/ABS(RUN)
DO 212 I=1,51
202  AV(I)=SGN
CONTINUE
SIG=SEG*AKF/2.
DO 500 I=1,51
STR=FCAT(I)*SEF/2.
IF(I.EQ.51) STR=AES(RUN)
501  ANEUB=(STR*AKF)**2
Y1=SIG**2+SIG*(SIG/CSC)**(1./SHE)*E-ANEUB
Y2=2.*SIG*(1./SHE+1)*(SIG/CSC)**(1./SHE)*E
SIG=(Y1+Y2)
IF(AES(Y1).GT.0.01*ANEUB) GO TO 511
STRESS(I+1)=SIG
500  STRAIN(I)=SIG/E+(SIG/CSC)**(1./SHE)
CONTINUE
STRESS(1)=0.
STRS=STRESS(52)*SGN
ISTART=ISTART+1
IF(ISTART.GT.NPEAKS) ISTART=1
ISTOP=NPEAKS
DAMAGE=0.
300  DO 400 I=ISTART,ISTOP
J=0
SGN=1
IF(DATA(I).LT.RUN) SGN=-1.
301  J=J+1
RUN=RUN+SEG*SGN
STRS=STRS+(STRESS(J+1)-STRESS(J))*SGN*2.
AV(J)=SGN
IF(AV(J+1).NE.SGN) GO TO 350
SM=STRS-STRESS(J+1)*SGN
EST=(STRAIN(J)*E/(SF-SM))** (1./B)
302  Y1=STRAIN(J)-EF*EST**C-(SF-SM)/E*EST**B
Y2=-C*EF*EST** (C-1.)-E*(SF-SM)/E*EST** (B-1.)
EST=EST-Y1/Y2
IF(ABS(Y1).GT.0.01*STRAIN(J)) GO TO 302
DAMAGE=DAMAGE+2./EST
303  J=J+1
IF(J.GE.51) GO TO 400
IF(AV(J+1).EQ.SGN) GO TO 313
IF((DATA(I)-RUN)*SGN+0.01*SEG.GE.0.) GO TO 301
350  CONTINUE
400  IF(ISTART.EQ.1) GO TO 401
ISTOP=ISTART-1
ISTART=1
GO TO 300
401  DAMAGE=1./DAMAGE
TYPE 104,DAMAGE
104  FORMAT(' ELOCKS TO FAILURE ',E)
STOP
END
```


REFERENCES

1. W. R. Brose, N. E. Dowling and JoDean Morrow, "Effect of Periodic Large Strain Cycles on the Fatigue Behavior of Steels," Paper 740221 presented at SAE Automotive Engineering Congress, Detroit, Michigan, February, 1974.
2. N. E. Dowling, "Fatigue Failure Predictions for Complicated Stress-Strain Histories," Journal of Materials, JMSLA, Vol. 7, No. 1, March, 1972, pp. 71-87.
3. J. F. Martin, T. H. Topper and G. M. Sinclair, "Computer Based Simulation of Cyclic Stress-Strain Behavior with Applications to Fatigue," Materials Research and Standards, MTRSA, Vol. 11, No. 2, February, 1971, pp. 23-29.
4. R. M. Wetzel, "A Method of Fatigue Damage Analysis," Ph.D. Thesis, Department of Civil Engineering, University of Waterloo, Ontario, Canada, 1971.
5. F. D. Richards, N. R. LaPointe and R. M. Wetzel, "A Cycle Counting Algorithm for Fatigue Damage Analysis," Paper 740278 presented at SAE Automotive Engineering Congress, Detroit, Michigan, February, 1974.
6. R. W. Landgraf, F. D. Richards and N. R. LaPointe, "Fatigue Life Predictions for a Notched Member under Complex Load Histories," Paper 750040 presented at SAE Automotive Engineering Congress, Detroit, Michigan, February, 1975.
7. T. H. Topper, R. M. Wetzel and JoDean Morrow, "Neuber's Rule Applied to Fatigue of Notched Specimens," Journal of Materials, JMSLA, Vol. 4, No. 1, March, 1969, pp. 200-209.
8. S. J. Stadnick and JoDean Morrow, "Techniques for Smooth Specimen Simulation of the Fatigue Behavior of Notched Members," Testing for Prediction of Material Performance in Structures and Components, ASTM STP 515, 1972, pp. 229-252.
9. D. F. Socie, "Fatigue Life Prediction Using Local Stress-Strain Concepts," Paper presented at 1975 SESA Spring meeting, Chicago, Illinois, May, 1975.
10. Lee Tucker and Steve Bussa, "The SAE Cumulative Fatigue Damage Test Program," Paper 750038 presented at SAE Automotive Engineering Congress, Detroit, Michigan, February, 1975.
11. R. E. Peterson, Stress Concentration Factors, John Wiley and Sons, 1974.
12. M. R. Mitchell, "A Unified Predictive Technique for the Fatigue Resistance of Cast Ferrous-Based Metals and High Hardness Wrought Steels," FCP Report No. 23, September, 1976
13. Y. Higashida and F. V. Lawrence, "Strain Controlled Fatigue Behavior of Weld Metal and Heat-Affected Base Metal in A36 and A514 Steels Welds," FCP Report No. 22, August, 1976.

Suspension History

Man-Ten			RQC-100		
Test	Maximum Load	Blocks to Initiation	Test	Maximum Load	Blocks to Initiation
SM1	- 16,000	7.7 - 28	SR 1	- 16,000	19.9 - 64
SM2	- 9,000	162 - 430	SR 2	- 9,000	1,710
SM3	- 6,000	1,410 - 2,240	SR 3	- 7,000	11,200
SM4	- 4,500	4,700	SR 4	- 6,000	48,000
SM5	- 3,000	> 85,370			

Bracket History

BM1	- 16,000	1.5 - 2	BR 1	- 16,000	3.3 - 5.1
BM2	- 8,000	11.5 - 23	BR 2	- 8,000	47 - 113
BM3	- 3,500	270 - 1,588	BR 3	- 3,500	2,673 - 5,020
BM4	- 3,000	2,666			
BM5	- 2,000	> 20,630			

Transmission History

TM1	+16,000	8.4 - 12.8	TR 1	+16,000	22.2 - 29.9
TM2	+ 8,000	74 - 420	TR 2	+ 8,000	269 - 460
TM3	+ 3,500	3,755 - 5,800	TR 3	+ 3,500	> 88,020

TABLE I

SUMMARY OF SAE CUMULATIVE FATIGUE DAMAGE TEST PROGRAM

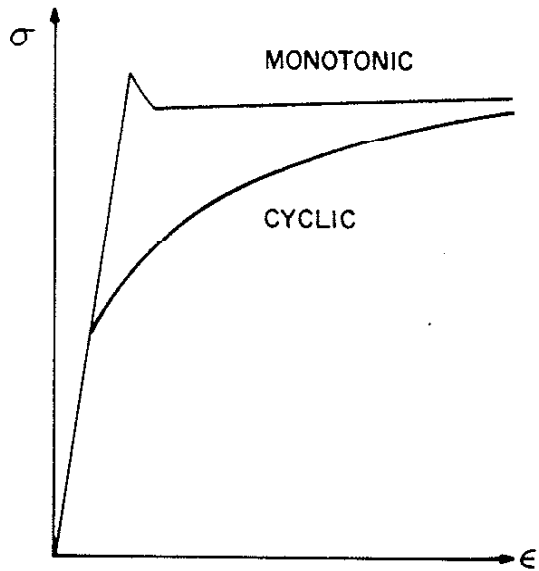
<u>Monotonic Properties</u>		<u>Man-Ten</u>	<u>RQC-100</u>
Elastic Modulus,	E	30×10^3 ksi	30×10^3 ksi
Yield Strength,	S_y	47 ksi	120 ksi
Tensile Strength,	UTS	82 ksi	125 ksi
Reduction in Area,	% RA	65%	55%
True Fracture Strength,	σ_f	145 ksi	173 ksi
True Fracture Ductility,	ϵ_f	1.19	0.78
Strength Coefficient,	K	140 ksi	174 ksi
Strain Hardening Exponent,	n	0.21	0.08

<u>Cyclic Properties</u>			
Fatigue Ductility Coefficient,	ϵ_f'	0.26	1.06
Fatigue Ductility Exponent,	c	-0.47	-0.75
Fatigue Strength Coefficient,	σ_f'	133 ksi	168 ksi
Fatigue Strength Exponent,	b	-0.095	-0.075
Cyclic Strength Coefficient,	K'	174 ksi	167 ksi
Cyclic Strain Hardening Exponent,	n'	0.20	0.10
Cyclic Yield Strength,	S_y'	48 ksi	85 ksi

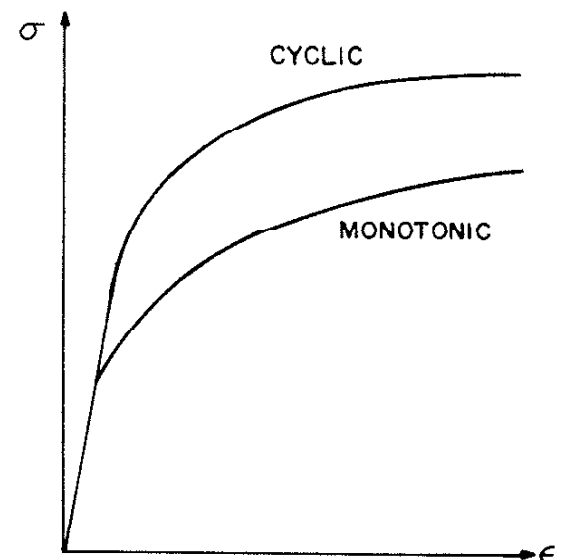
TABLE II
MECHANICAL PROPERTIES OF MAN-TEN AND RQC-100

<u>Test</u>	<u>Actual</u>	Nominal Strain Life	Load-Strain Analysis	Load-Stress Strain Analysis	Neuber Notch Analysis $K_f = 2.6$
SM1	7.7 - 28	93	33	34	27
SM2	162 - 430	940	480	506	455
SM3	1,410 - 2,240	5,890	3,642	3,988	4,590
SM4	4,700	25,940	18,010	20,750	32,100
SM5	> 85,370	335,000	270,000	347,000	915,000
BM1	1.5 - 2	5	1.3	1.2	1.0
BM2	11.5 - 23	54	27	25	22
BM3	270 - 1,588	3,053	2,225	2,000	3,335
BM4	2,666	8,110	6,230	5,524	10,790
BM5	> 20,630	166,000	146,000	123,000	356,000
TM1	8.4 - 12.8	42	10	10	8
TM2	74 - 420	468	218	200	168
TM3	3,755 - 5,800	21,470	15,422	13,410	21,440
SR1	19.9 - 64	56	42	42	38
SR2	1,710	687	599	689	1,210
SR3	11,200	3,590	3,366	4,564	16,920
SR4	48,000	14,310	14,283	22,920	123,000
BR1	3.3 - 5.1	2	1.4	1.3	1.1
BR2	47 - 113	39	34	30	49
BR3	2,673 - 5,020	73,000	82,547	47,750	233,000
TR1	22.2 - 29.9	19	13	12	10
TR2	269 - 460	261	225	200	301
TR3	> 88,020	650,000	753,000	276,000	1.4 E 7

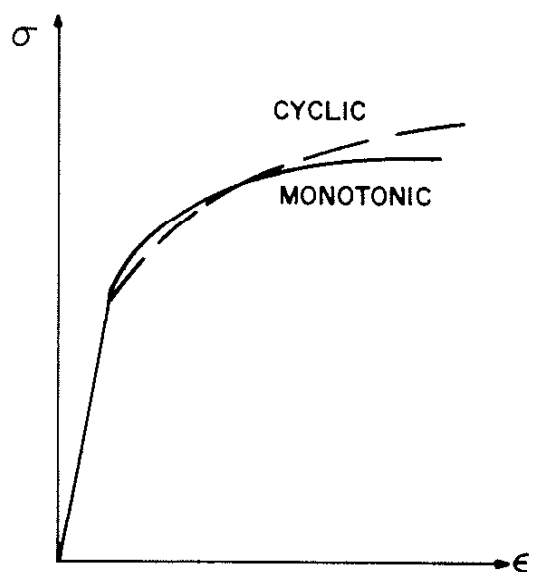
TABLE III
STRAIN LIFE ANALYSIS SAE KEYHOLE SPECIMEN



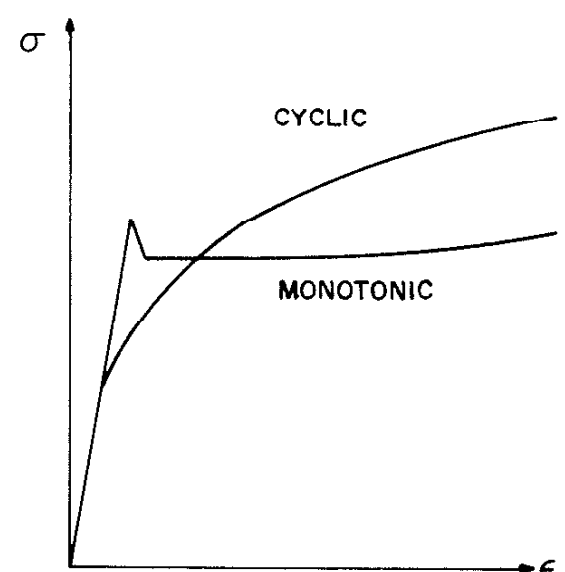
CYCLIC SOFTENING
RQC 100



CYCLIC HARDENING
304 STAINLESS STEEL



CYCLICALLY STABLE
2014-T6



MIXED BEHAVIOR
MANTEN

Fig. 1

CYCLIC AND MONOTONIC
STRESS-STRAIN BEHAVIOR OF METALS

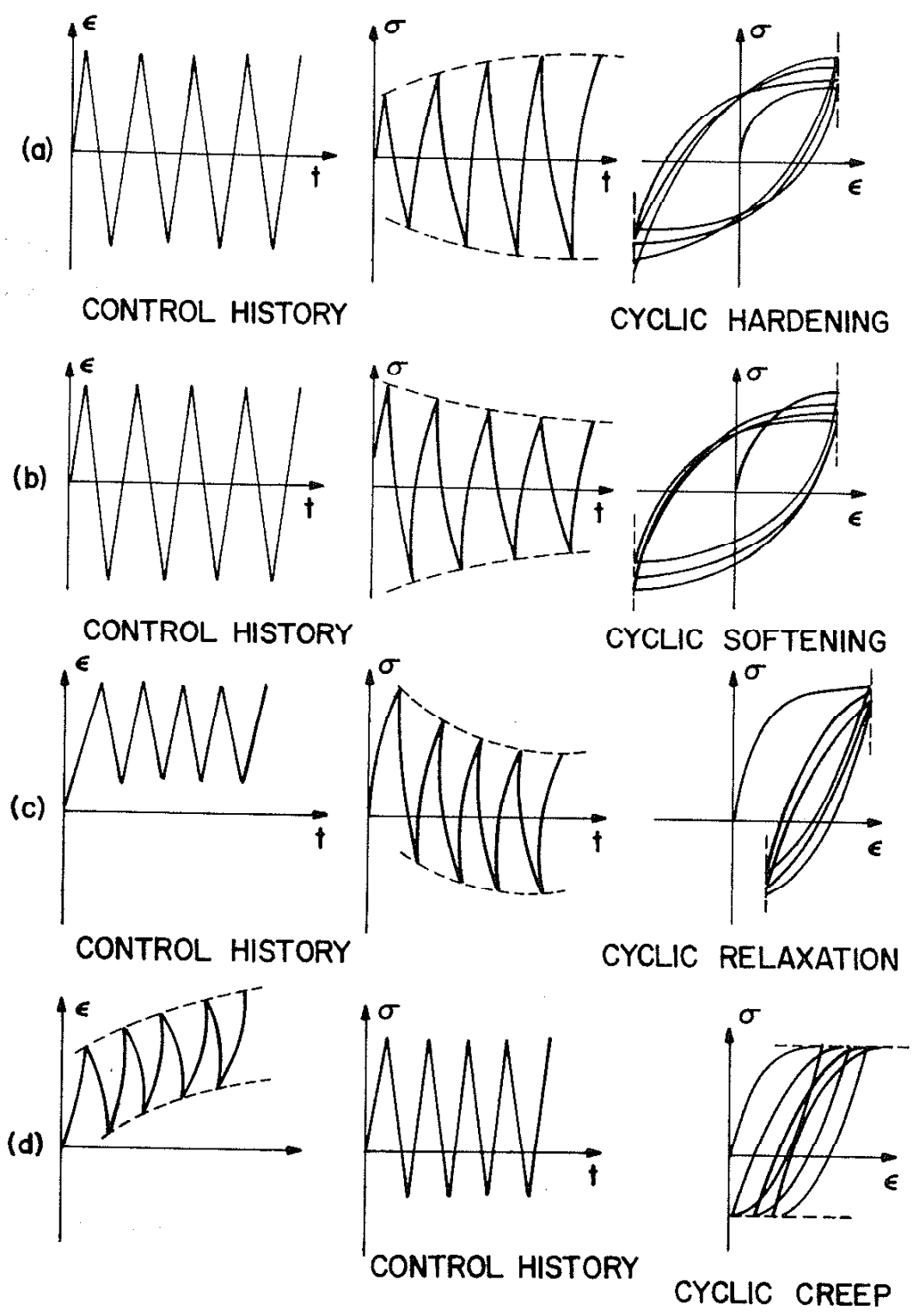


Fig. 2 Schematic Illustrations of Cyclic Transient Phenomena

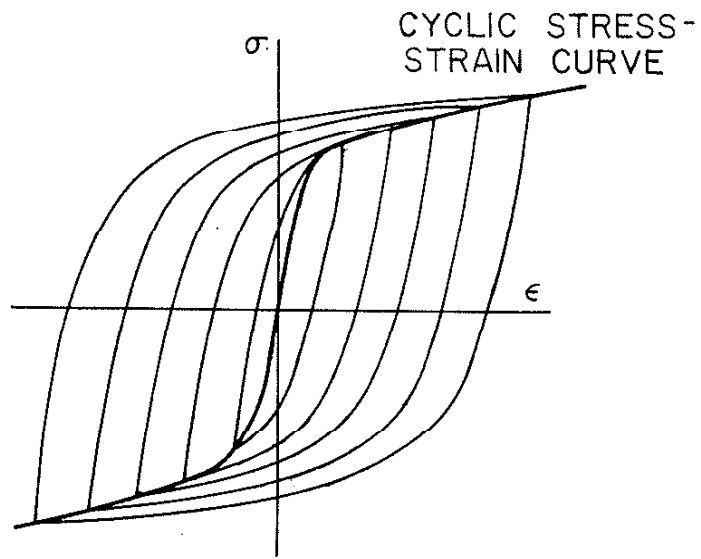
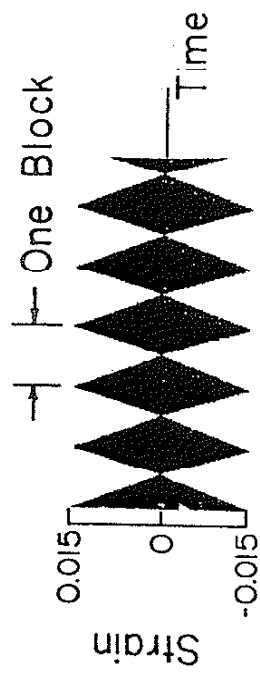
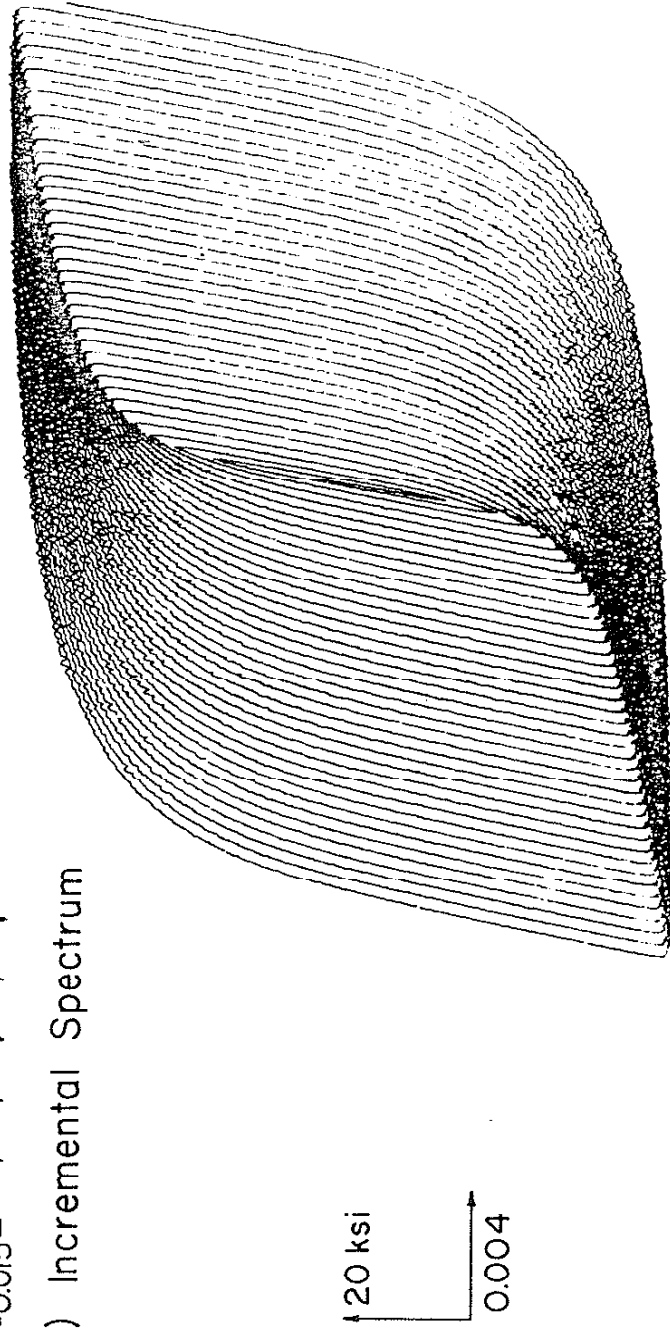


Fig. 3 Cyclic Stress-Strain Curve Drawn Through Stable Loop Tips



(a) Incremental Spectrum



(b) Stress-Strain Response (Decreasing Steps)

Fig. 4 Incremental Step Straining of Sheet Steel

Elastic Modulus = 29,700 KSI

N' = .092958	K' = 135.106	KSI	FROM LCF TESTS
N' = .138	K' = 174.3	KSI	FROM INCREM STEP
N' = .132	K' = 161.9	KSI	FROM TENSION

——— SOLID LINE ——— PLOT FROM LCF TEST
 - - - MARKED LINE - - - PLOT FROM INCREMENTAL STEP TEST
 - - - MARKED LINE - - - PLOT FROM TENSION AFTER CYCLING

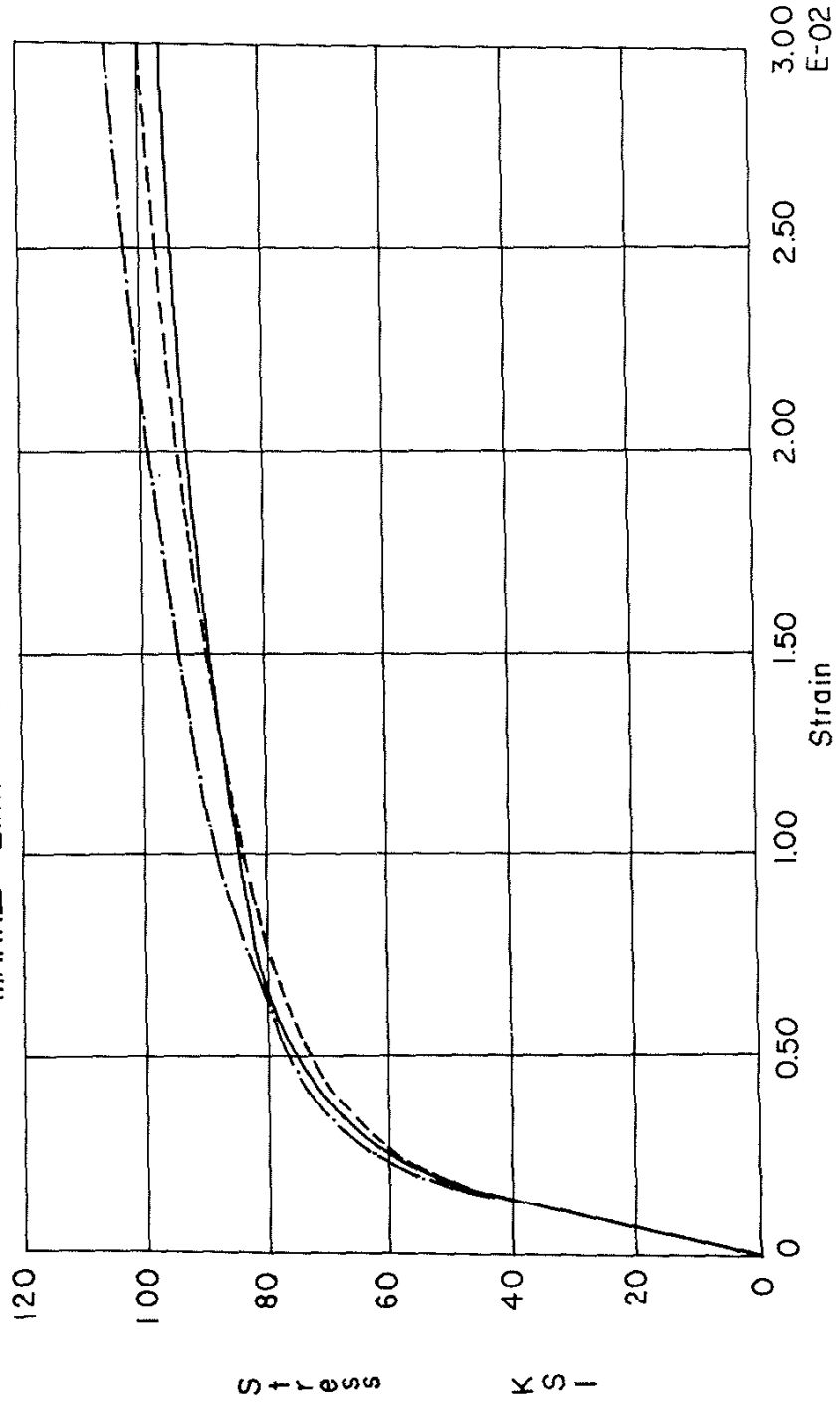


Fig. 5 Cyclic Stress - Strain Curves For RQC-100 Steel

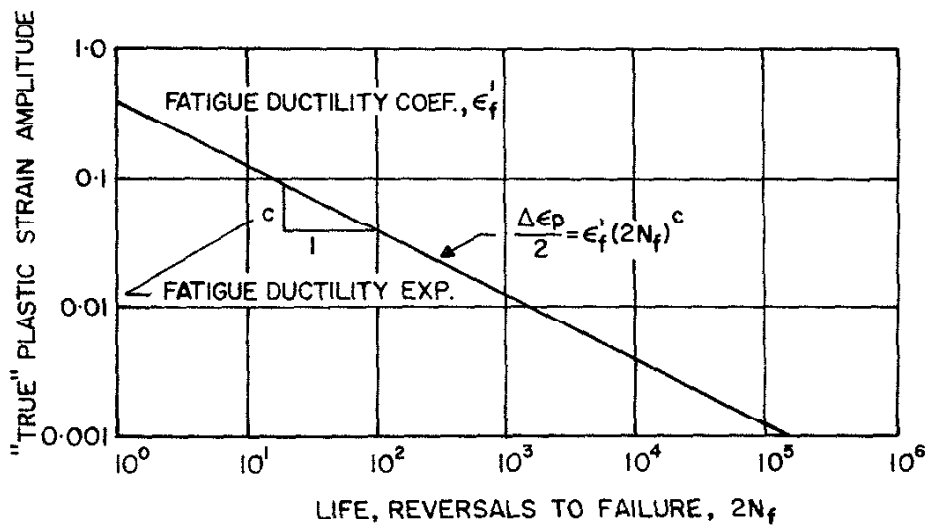


Fig. 6 PLASTIC STRAIN-LIFE CURVE

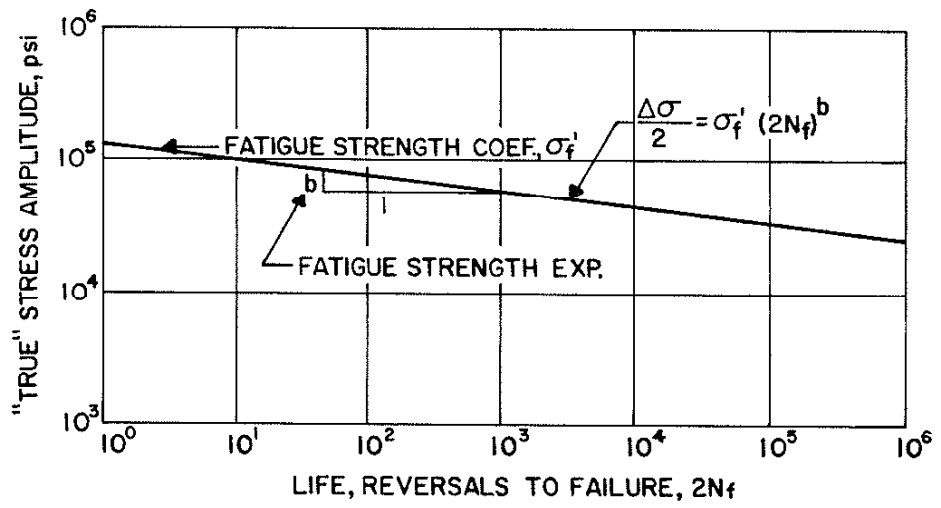
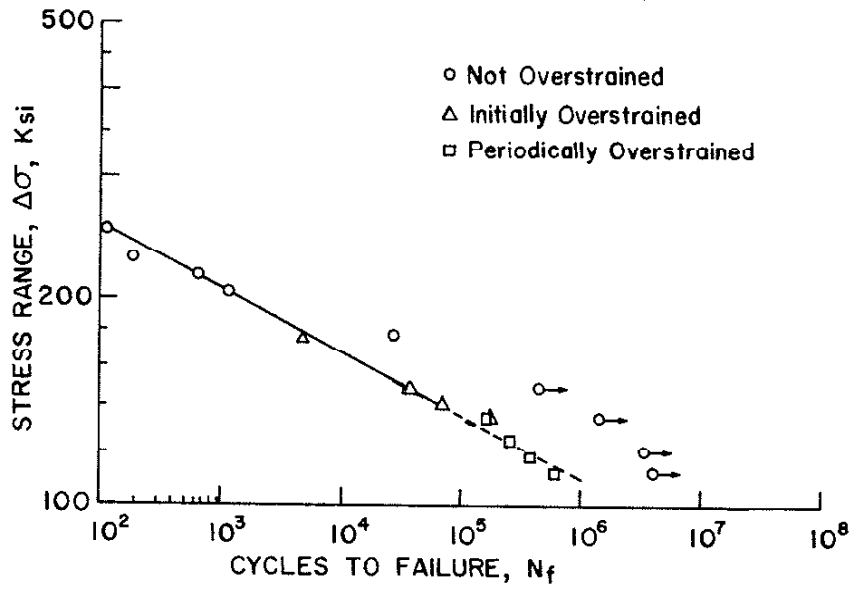
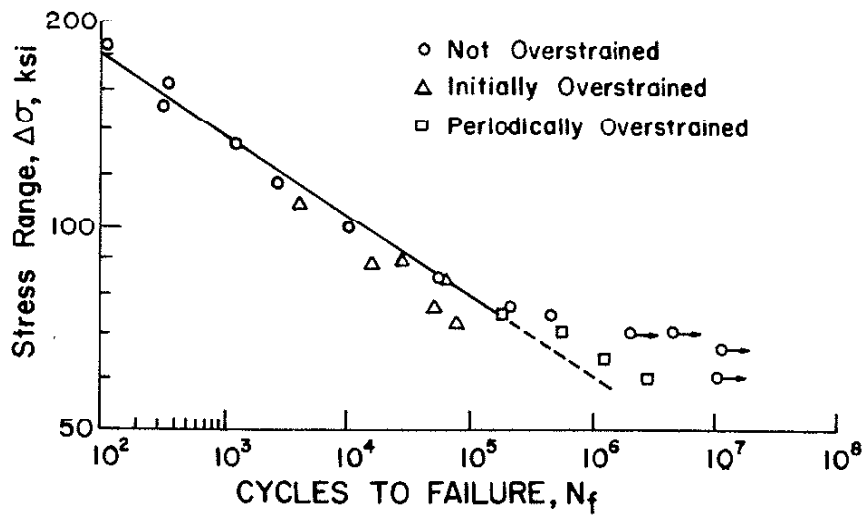


Fig. 7 STRESS-LIFE CURVE

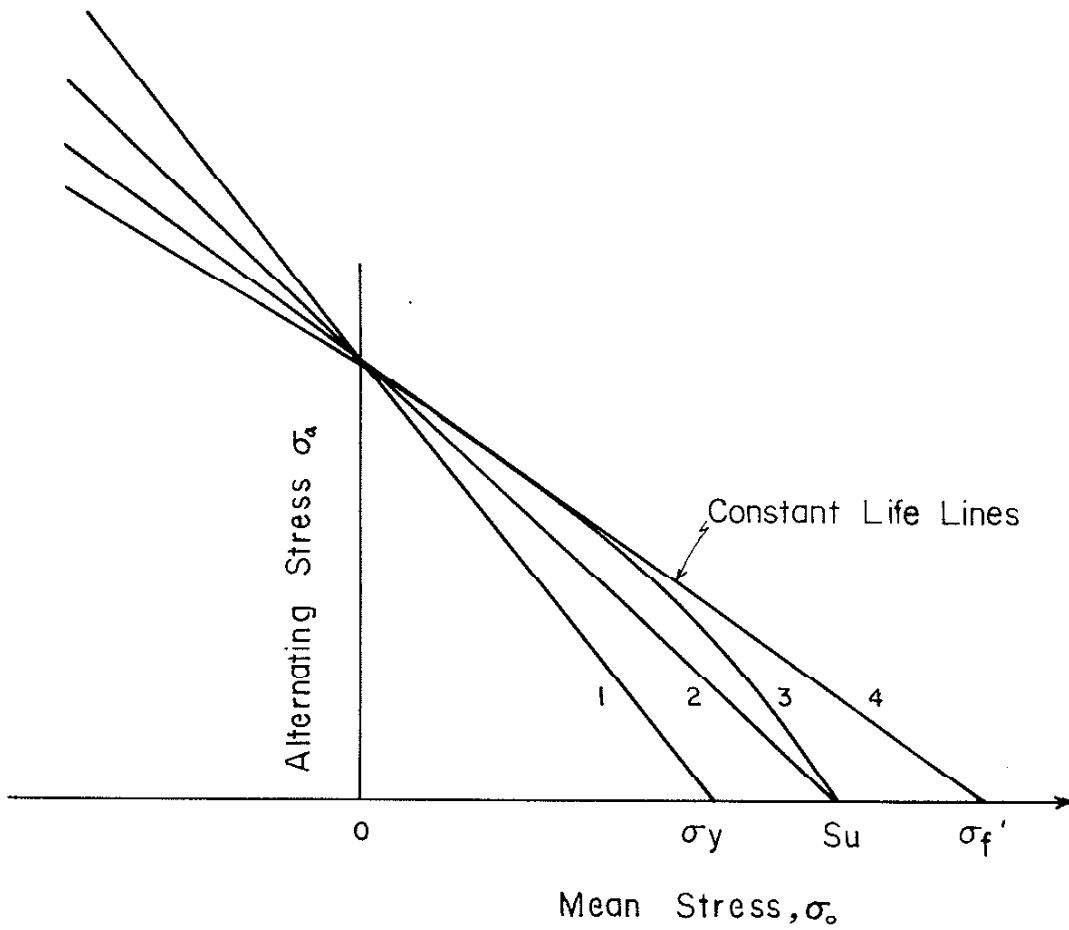


RQC-100



MANTEN

Fig. 8 EFFECT OF OVERSTRAIN ON THE FATIGUE BEHAVIOUR OF RQC-100 AND MANTEN (Ref.1)



- 1 Soderberg
- 2 Goodman
- 3 Gerber
- 4 Morrow

Fig. 9 Mean Stress Corrections

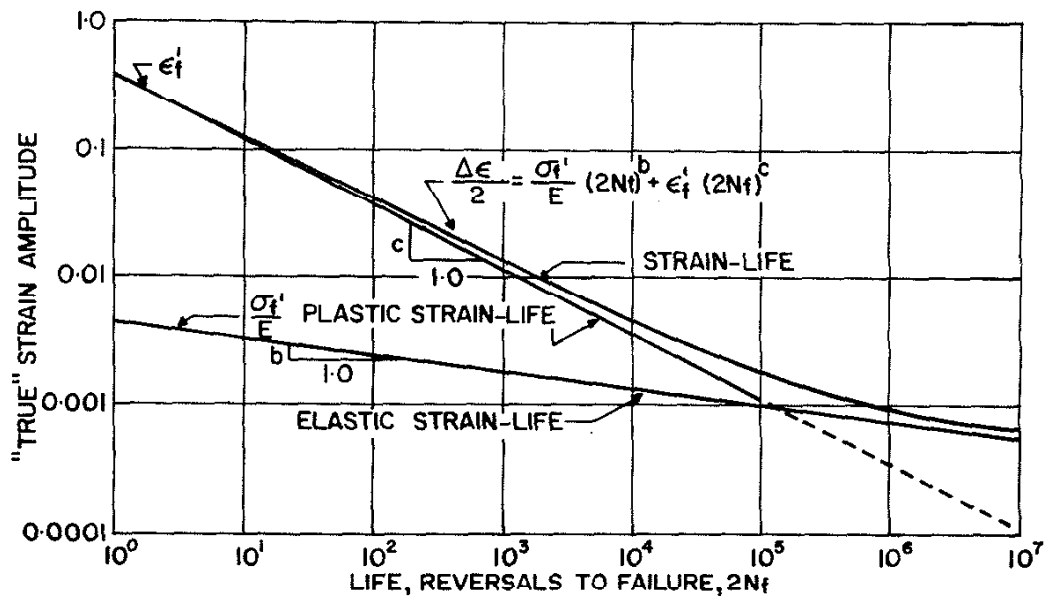


Fig. 10 TOTAL STRAIN-LIFE CURVE

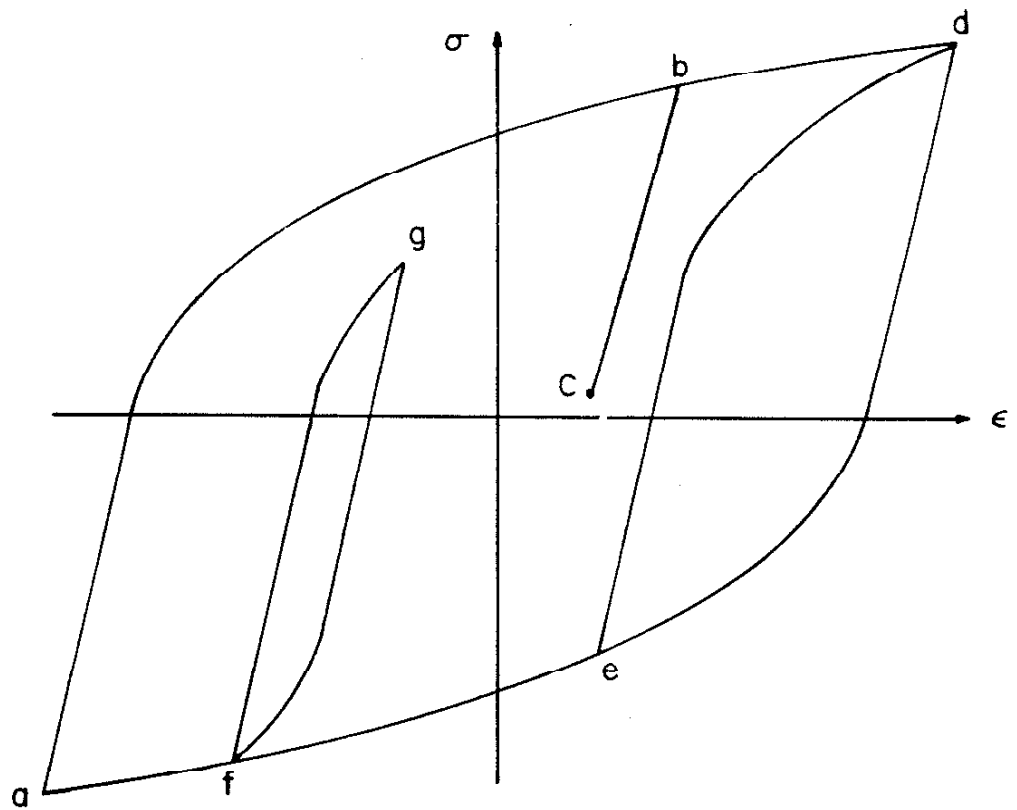
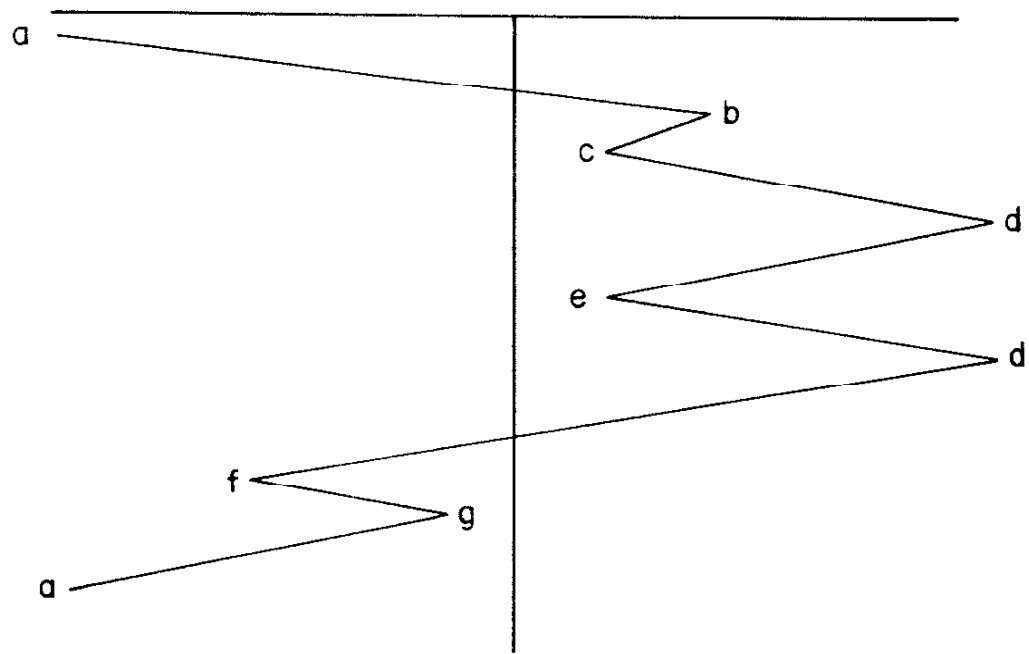
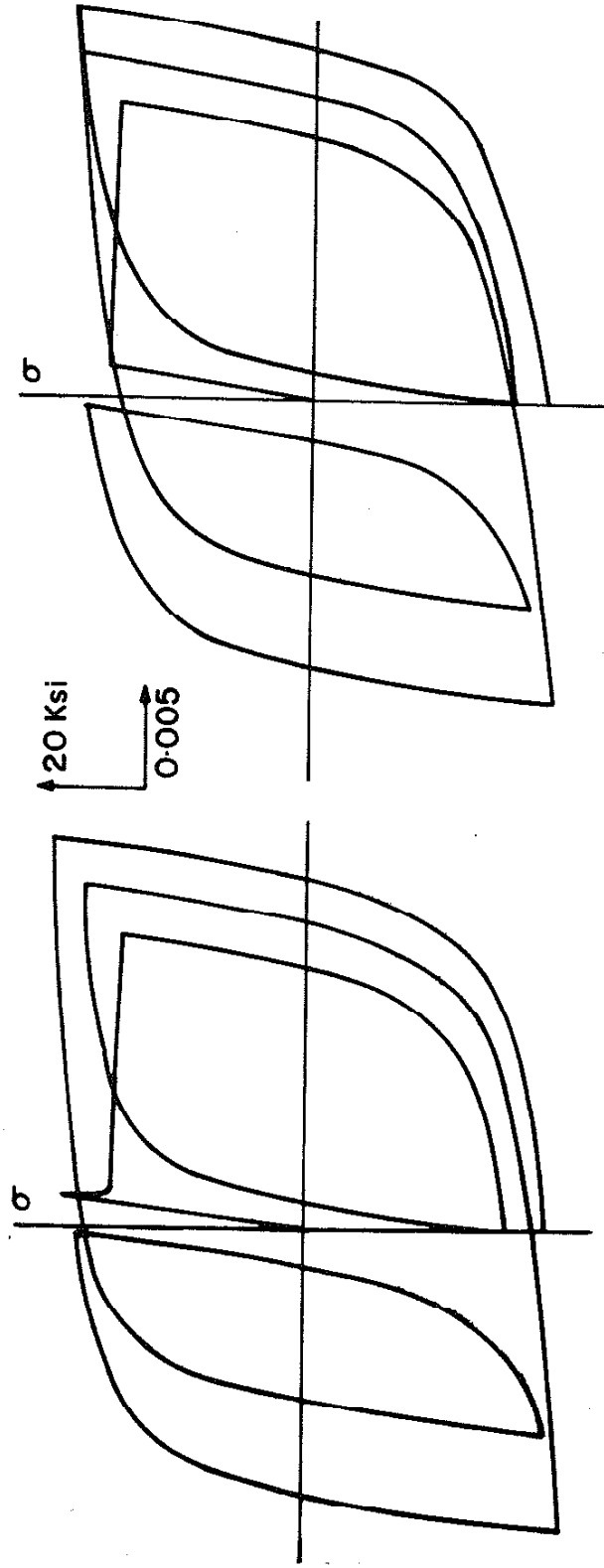


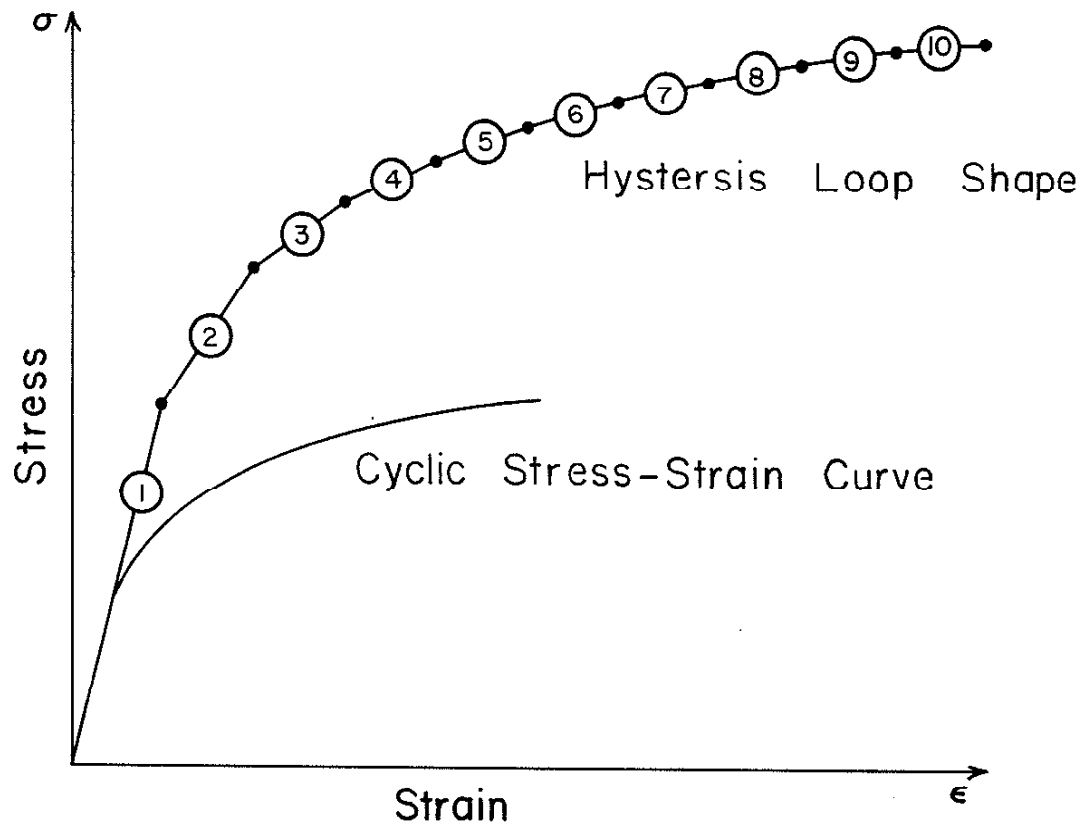
Fig. 11 STRESS-STRAIN RESPONSE DURING AN IRREGULAR LOADING HISTORY



(a) Test Results

(b) Simulation

Fig. 12 Actual and Simulated Stress-Strain Response of A36 Steel
(Ref.3)



Element	Stress, $\Delta\sigma$	Strain, $\Delta\epsilon$
1	30	0.0015
2	12	0.0015
3	9	0.0015
4	7	0.0015
5	5	0.0015
6	3	0.0015
7	2	0.0015
8	2	0.0015
9	1	0.0015
10	1	0.0015

Fig. 13 Elemental Cyclic Stress — Strain Curve

Reversal

	a	b	c	d	e	d	f	g	a
1	-	+	-	+	-	+	-	+	-
2	-	+	+	⊕	-	+	-	+	-
3	-	+	+	⊕	-	+	-	-	⊖
4	-	+	+	⊕	-	+	-	-	⊖
5	-	+	+	⊕	+	⊕	-	-	⊖
6	-	+	+	⊕	+	⊕	-	-	⊖
7	-	+	+	⊕	+	⊕	-	-	⊖
8	-	-	-	+	+	⊕	-	-	⊖
9	-	-	-	+	+	⊕	+	+	-
10	-	-	-	+	+	⊕	+	+	-

○ Indicates Skipped Element

Fig. 14 Availability Matrix Used For Material Response Model

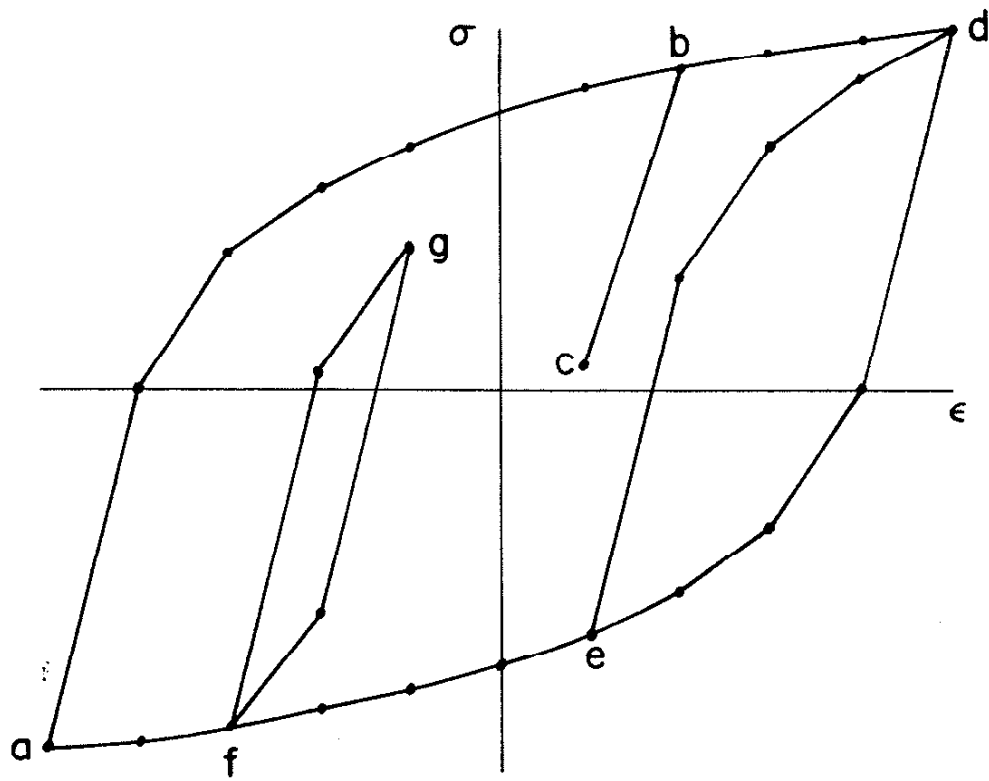
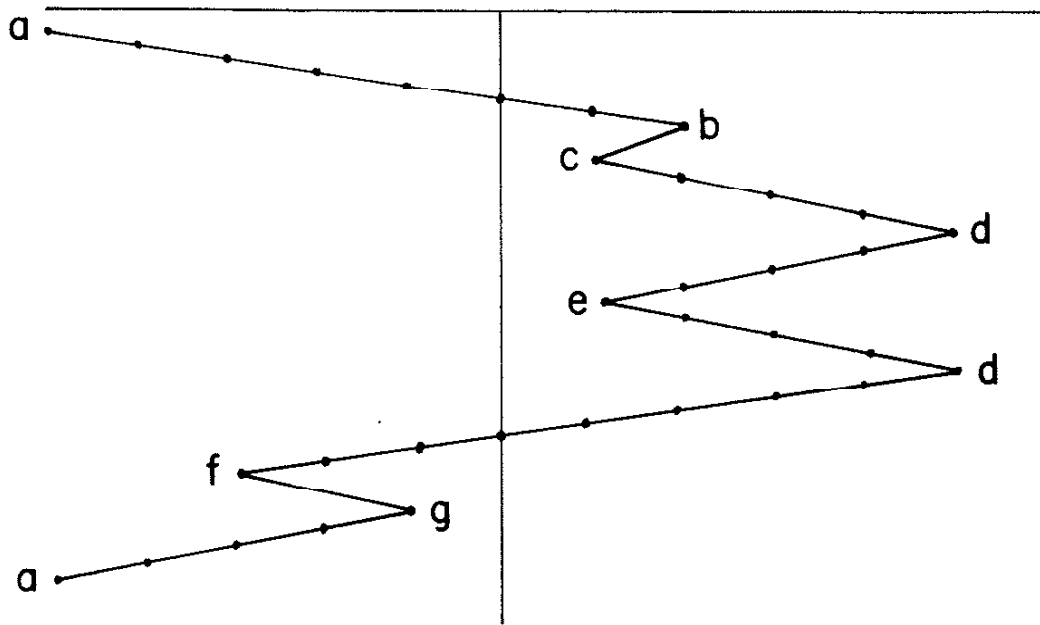


Fig. 15

Simulation Of Stress Strain Response For An Irregular Loading History

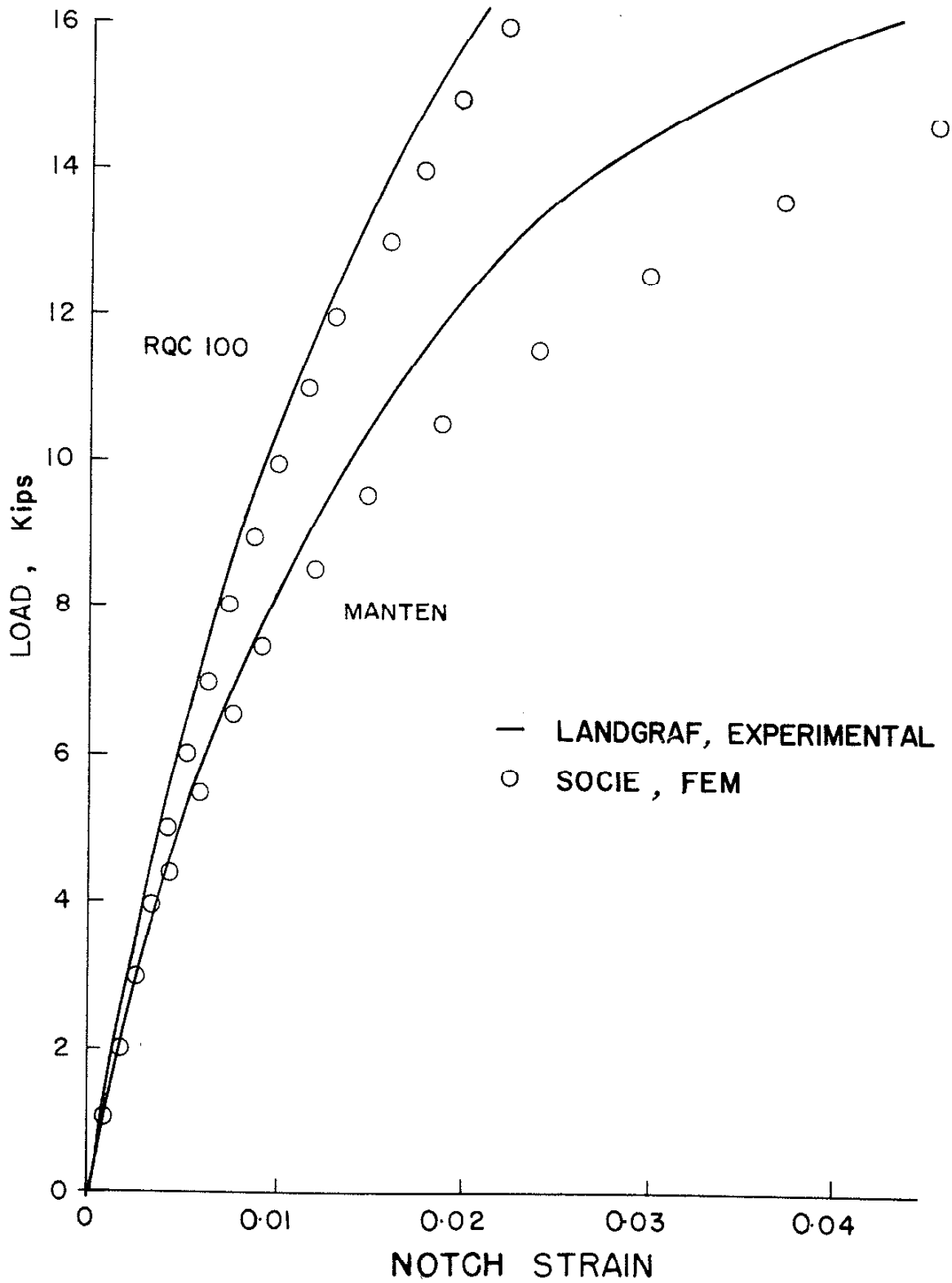


Fig. 16 LOAD-STRAIN CURVE FROM FINITE ELEMENT ANALYSIS

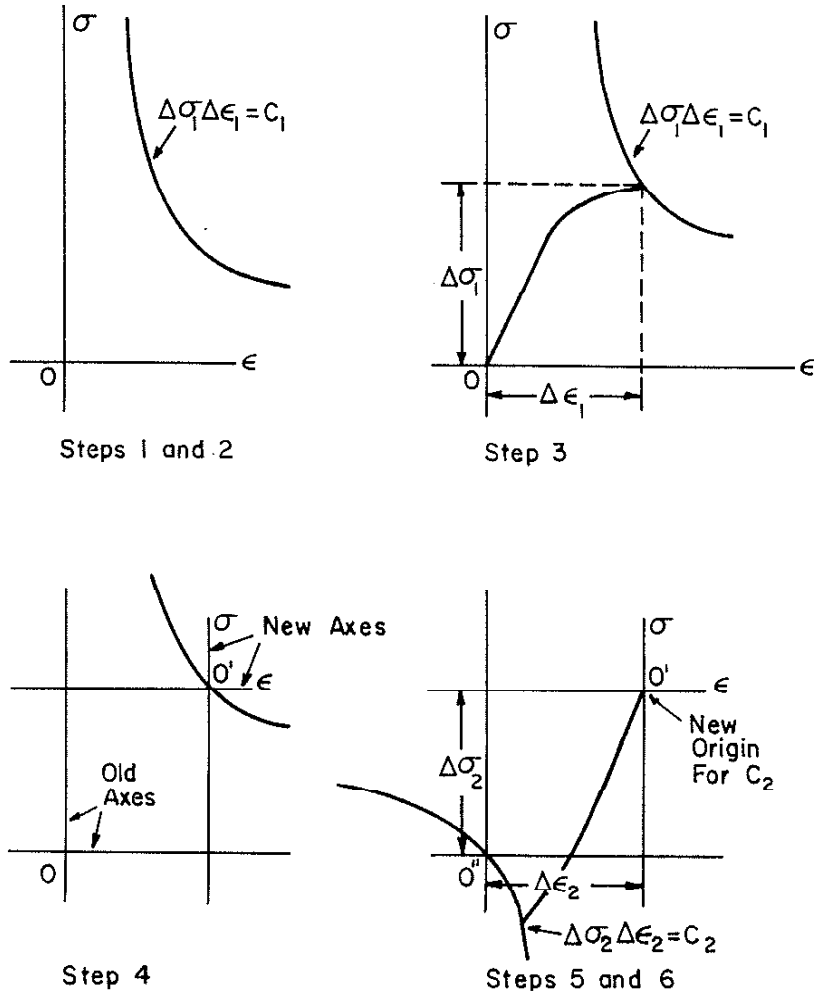


Fig. 17 Steps of Neuber Control

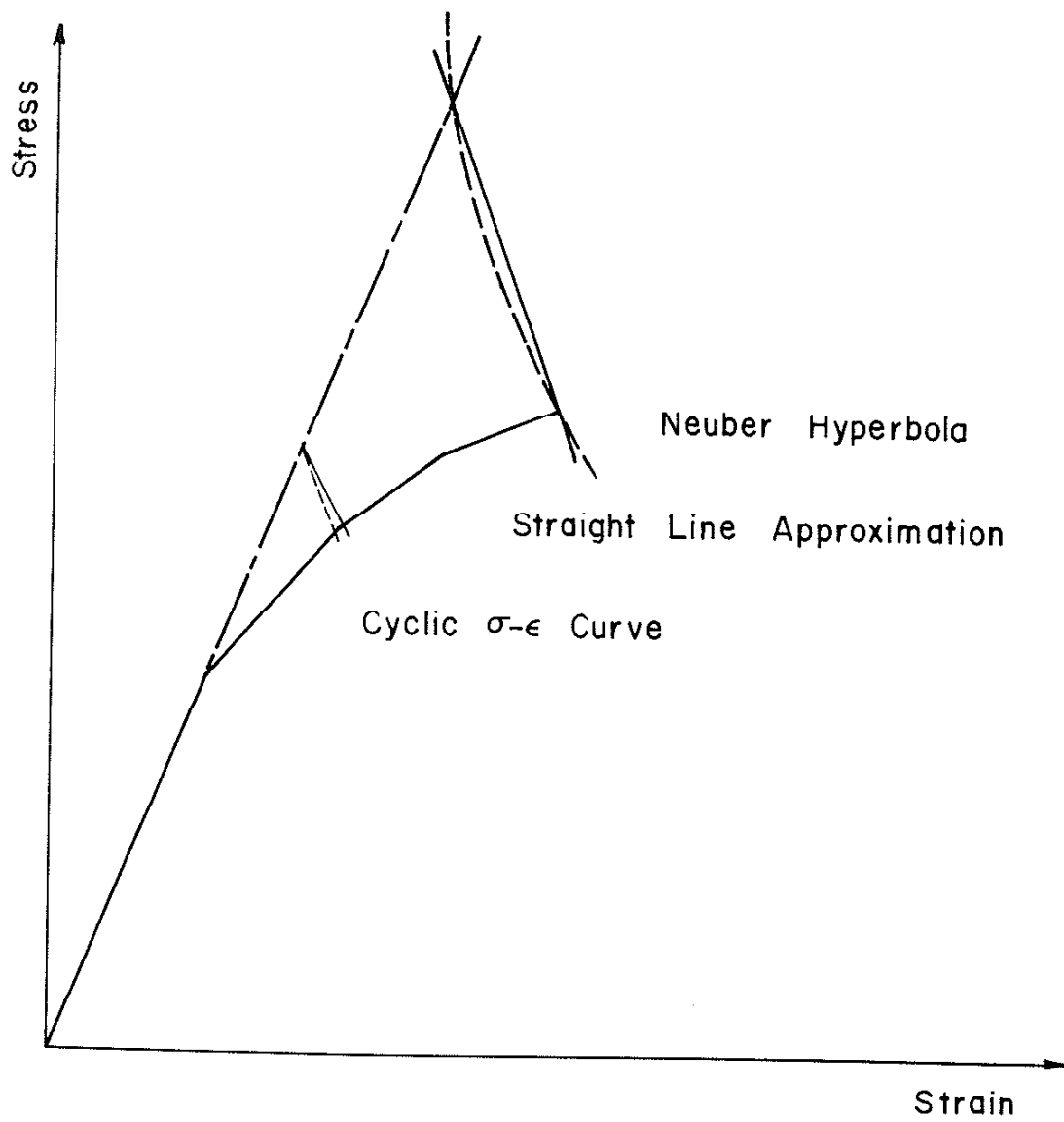


Fig. 18 Construction For Determining Notch Root Stress And Strain

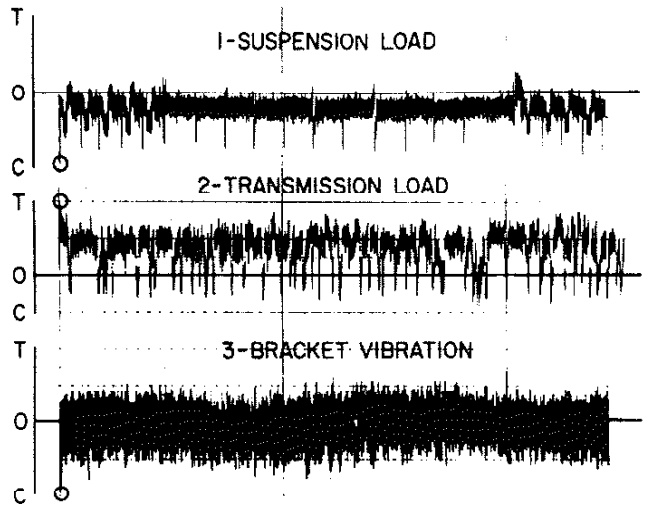


Fig. 19 SAE Load Histories

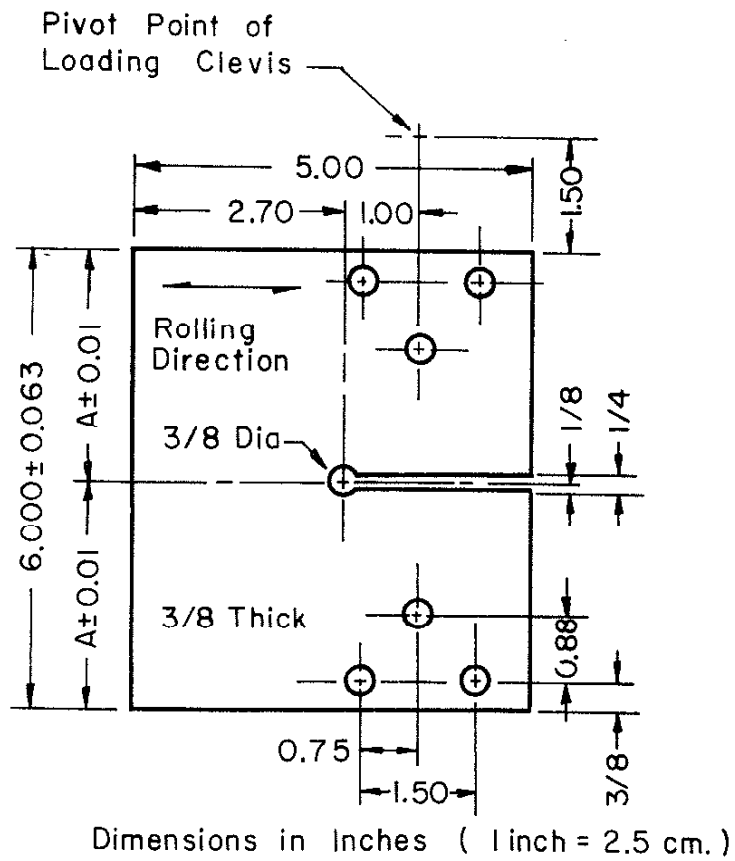


Fig. 20 Sketch of SAE Keyhole Specimen

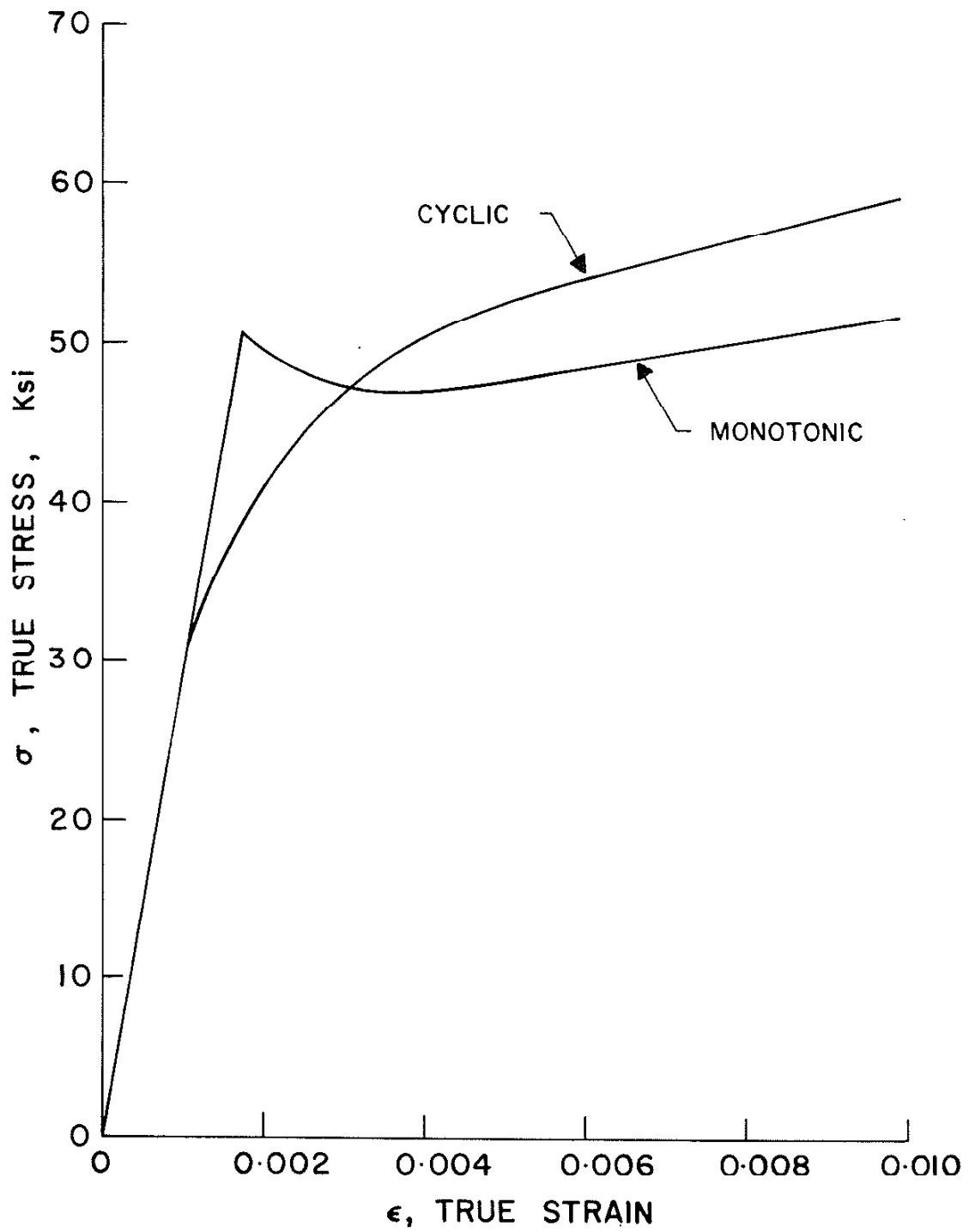


Fig. 21 STRESS - STRAIN CURVES FOR MANTEN

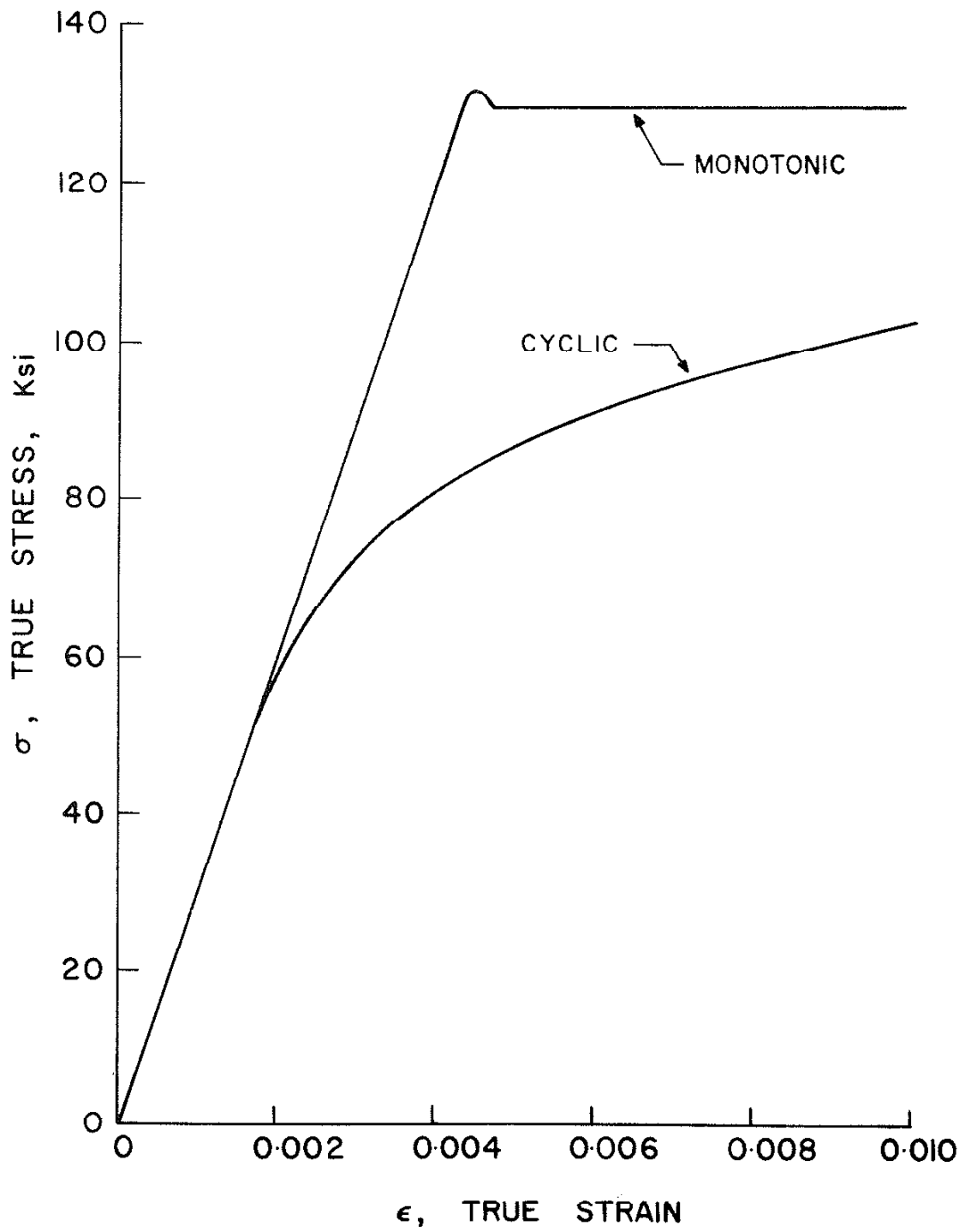


Fig. 22 STRESS STRAIN CURVES FOR RQC-100

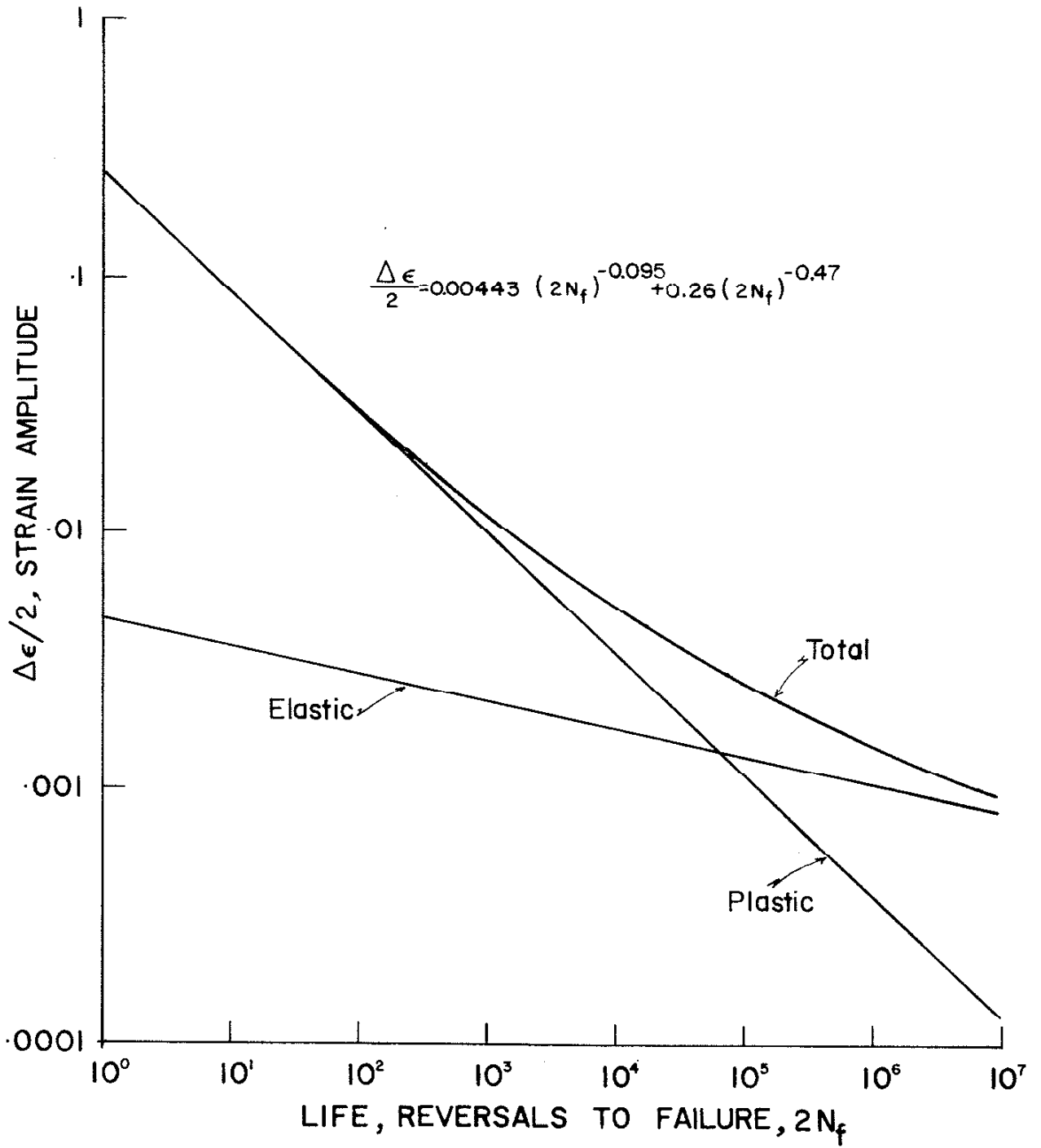


Fig. 23

STRAIN-LIFE CURVE FOR MANTEN

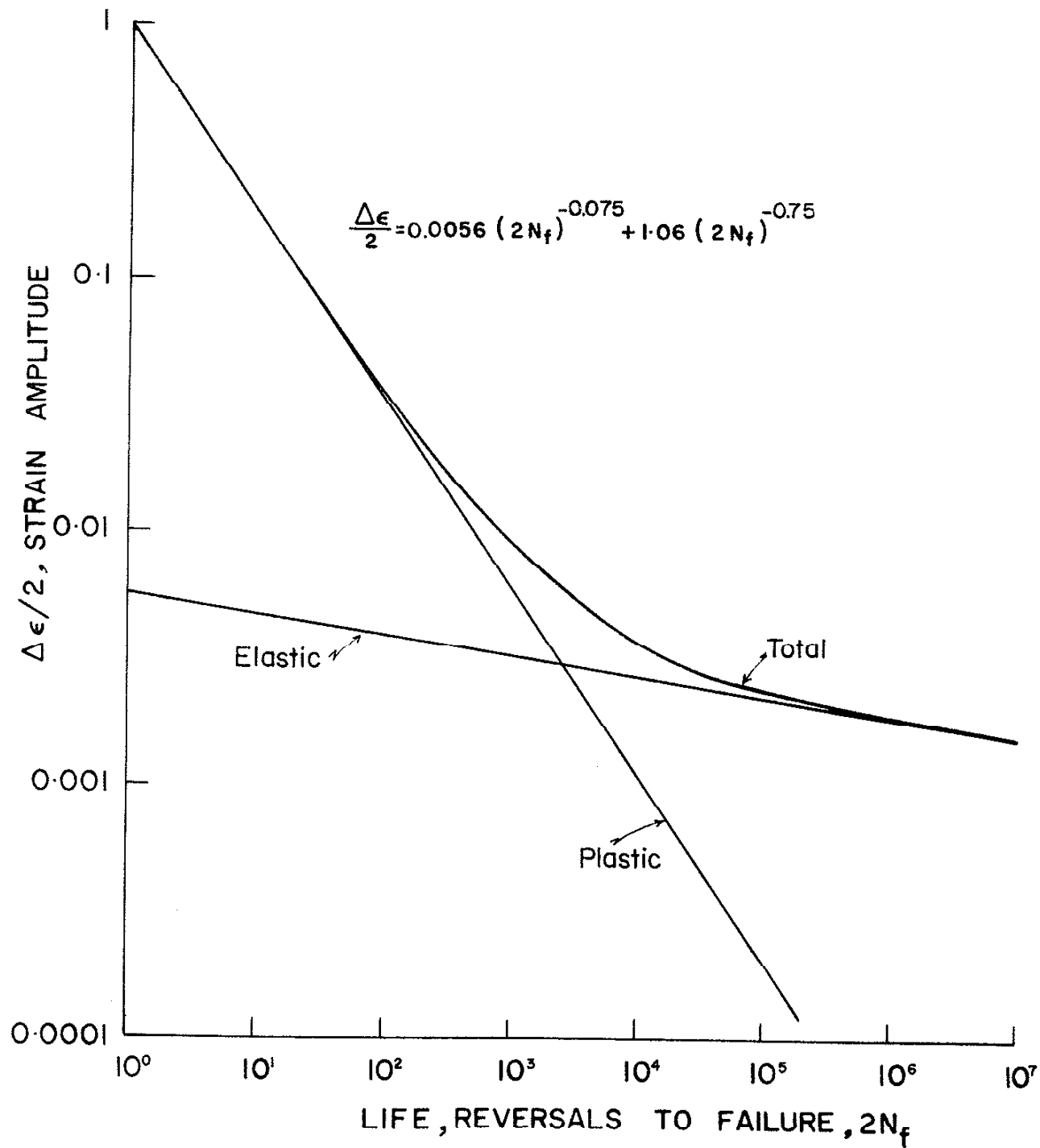


Fig. 24 STRAIN-LIFE CURVE FOR RQC-100

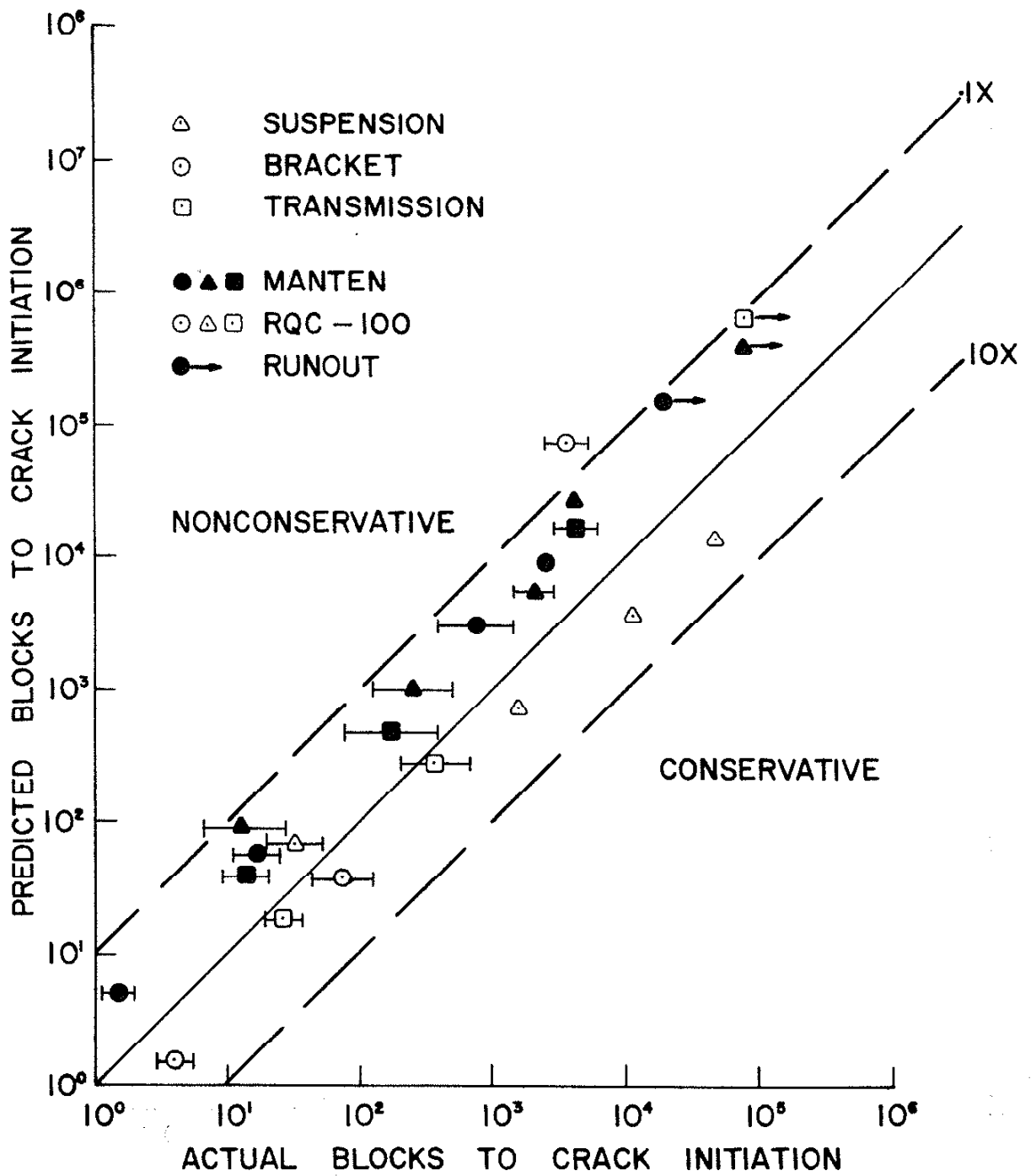


Fig. 25. NOMINAL STRAIN-LIFE ANALYSIS

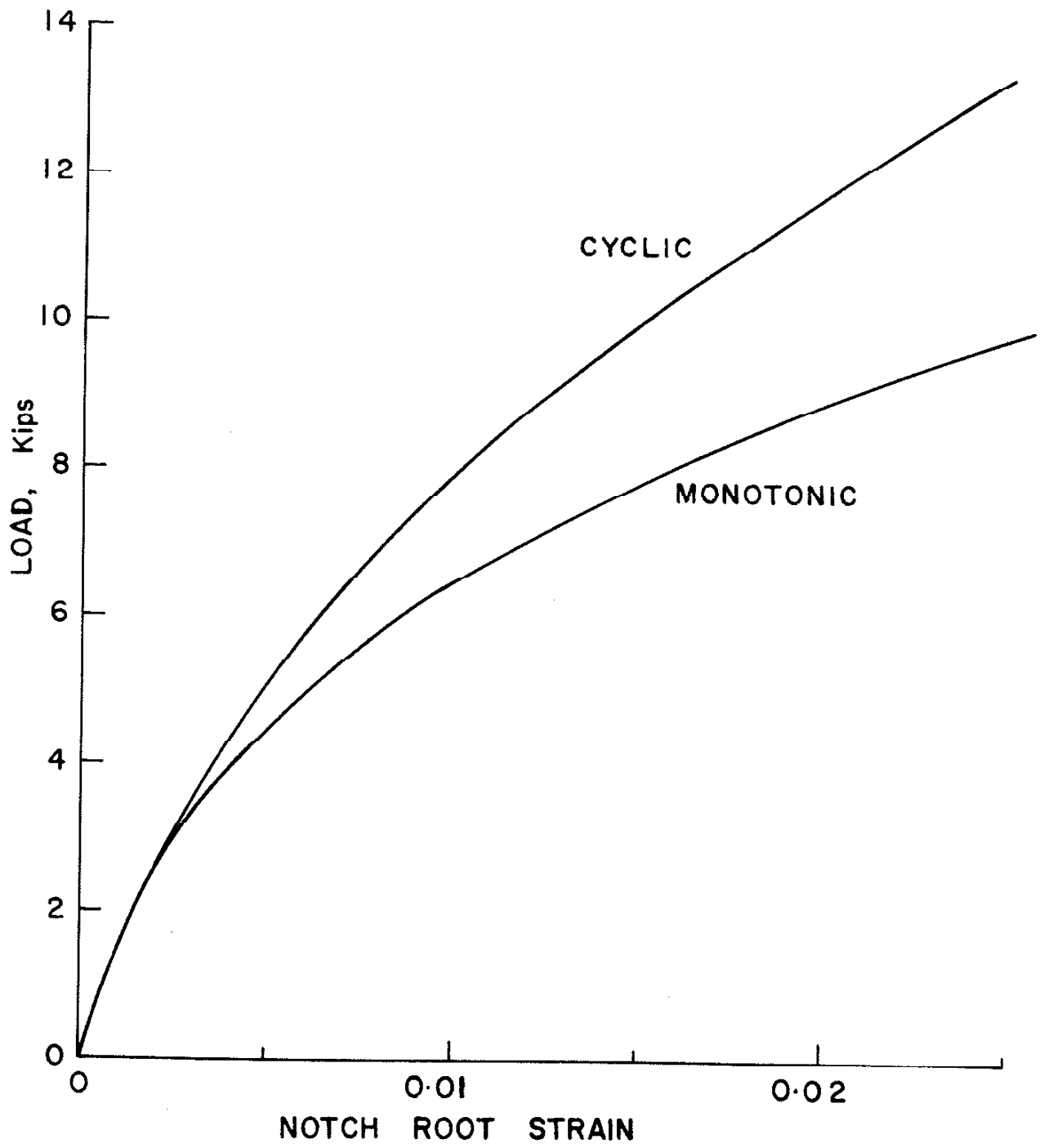


Fig. 26 | LOAD - NOTCH ROOT STRAIN FOR MANTEN

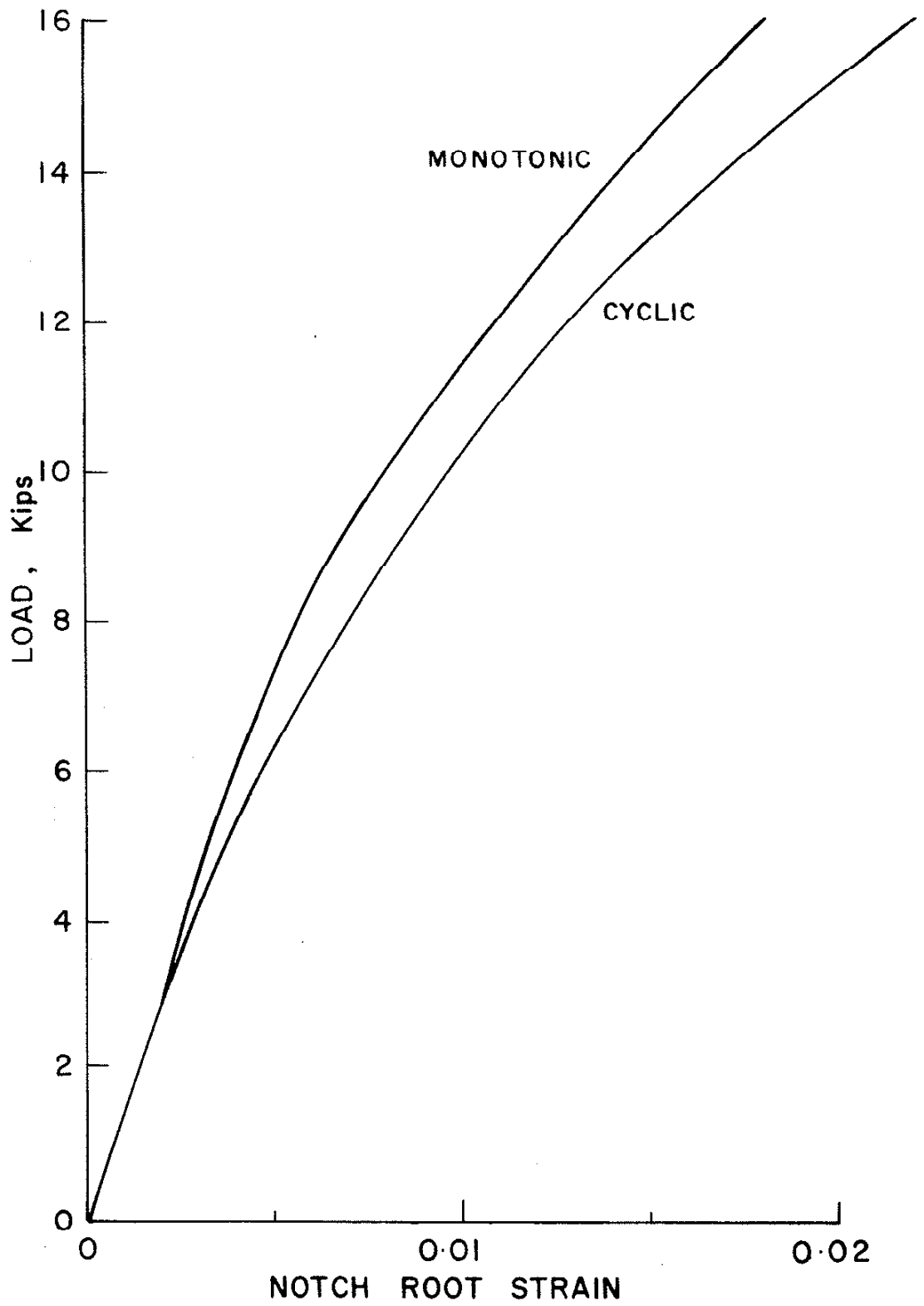


Fig. 27 LOAD - NOTCH ROOT STRAIN FOR RQC-100

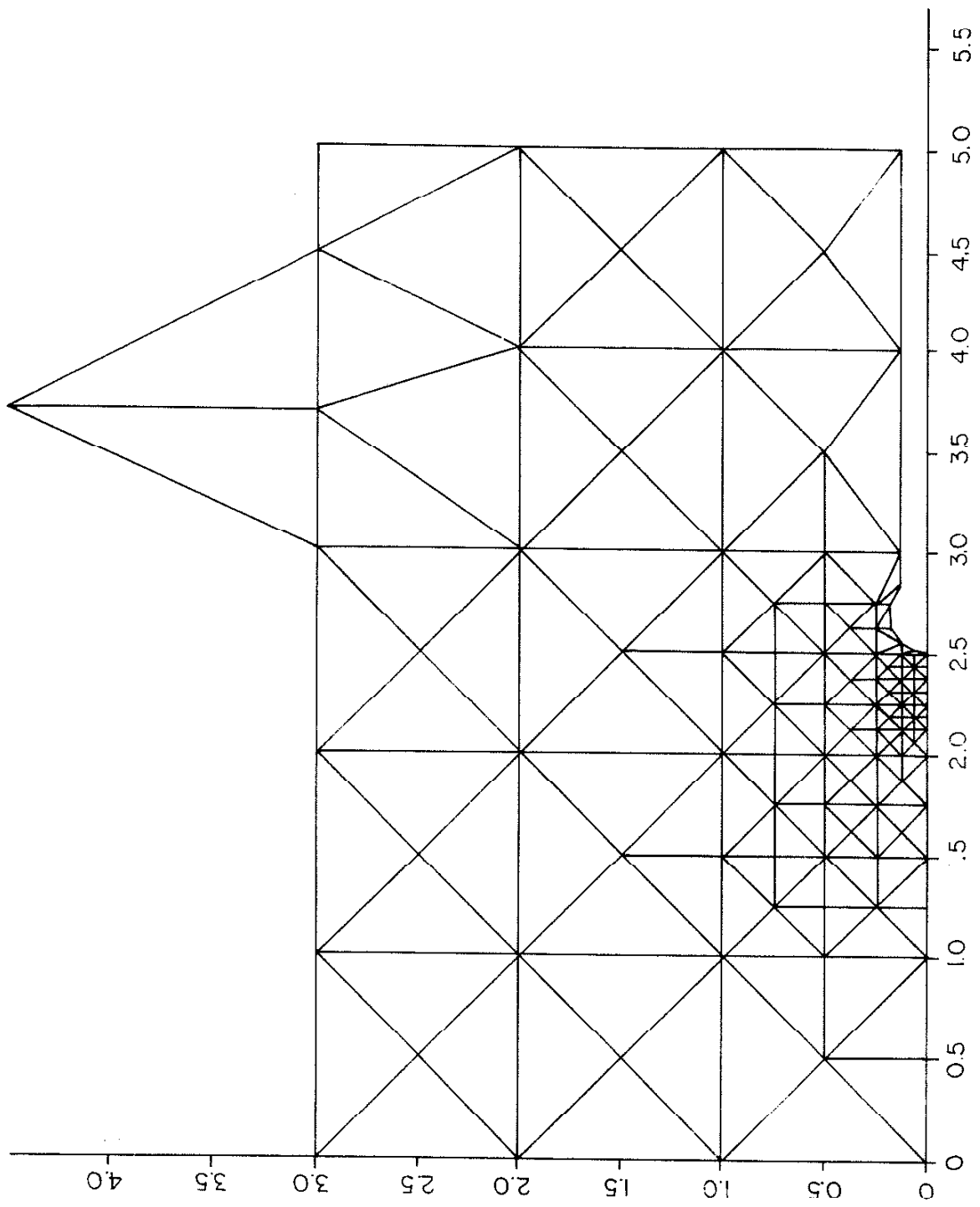


Fig. 28 Element Mesh for a Keyhole Notched Member (SAE Specimen)

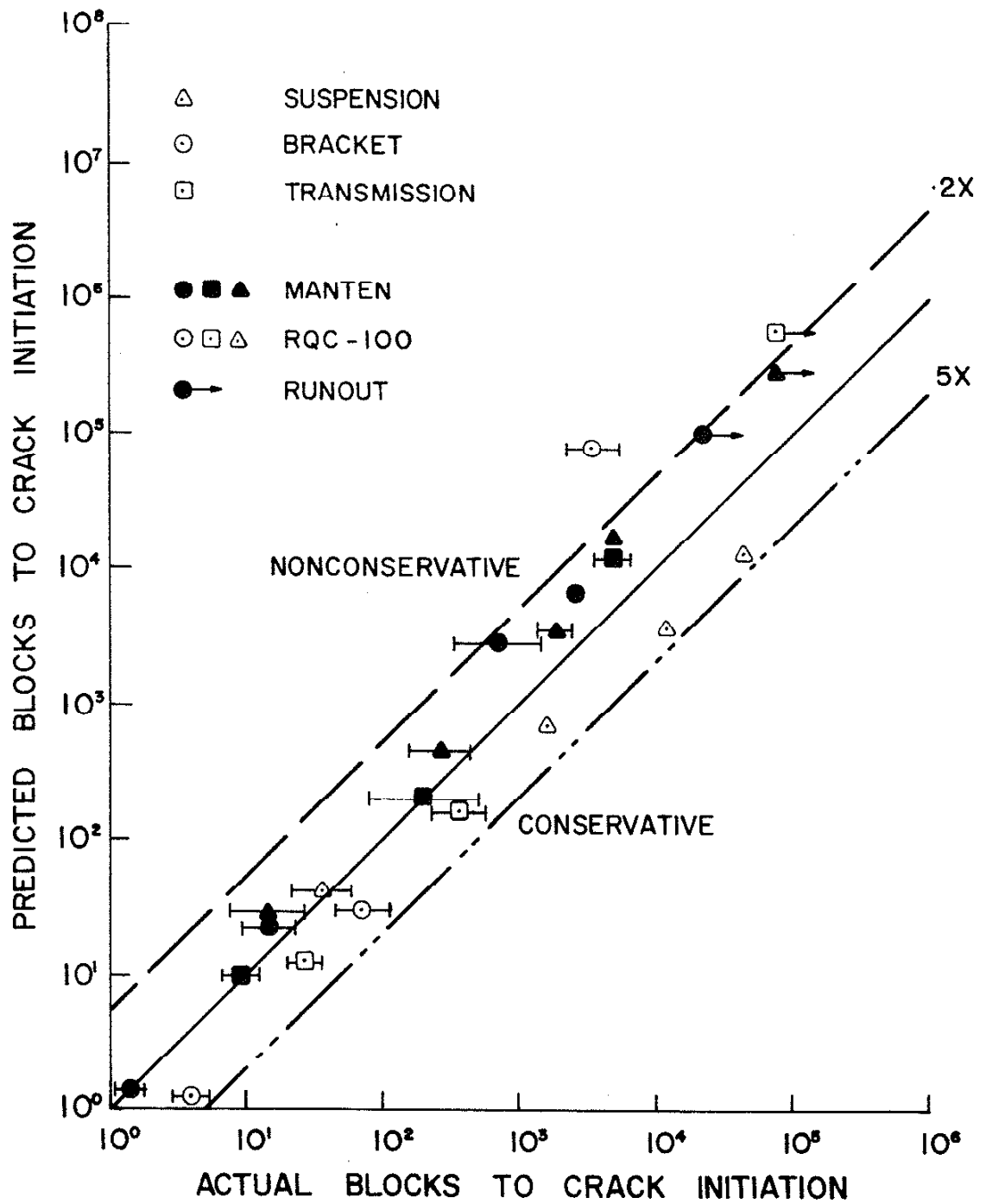


Fig. 29

LOAD-STRAIN ANALYSIS

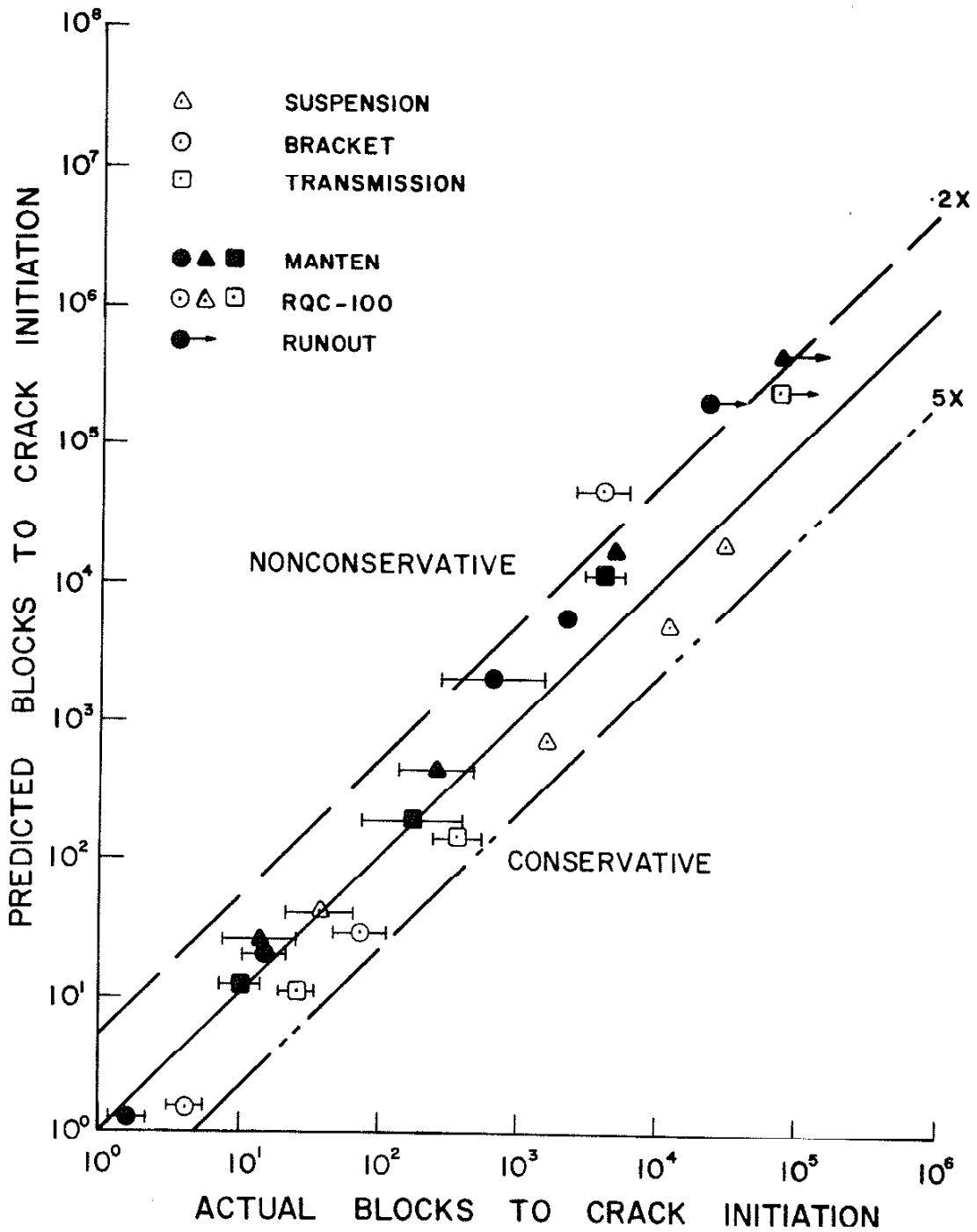


Fig. 30 LOAD-STRESS-STRAIN ANALYSIS

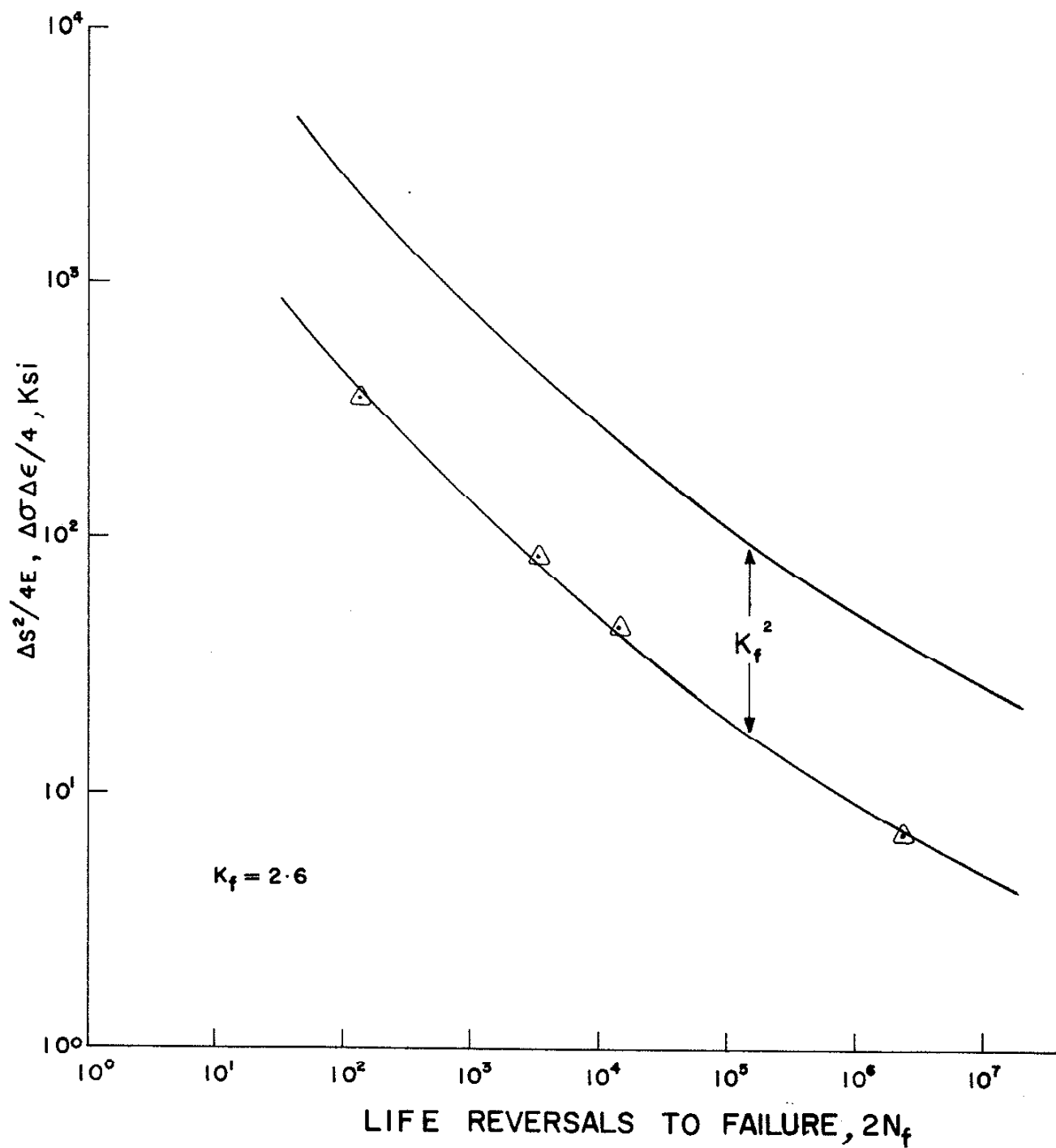


Fig. 31 NEUBER PLOT FOR MANTEN SPECIMEN

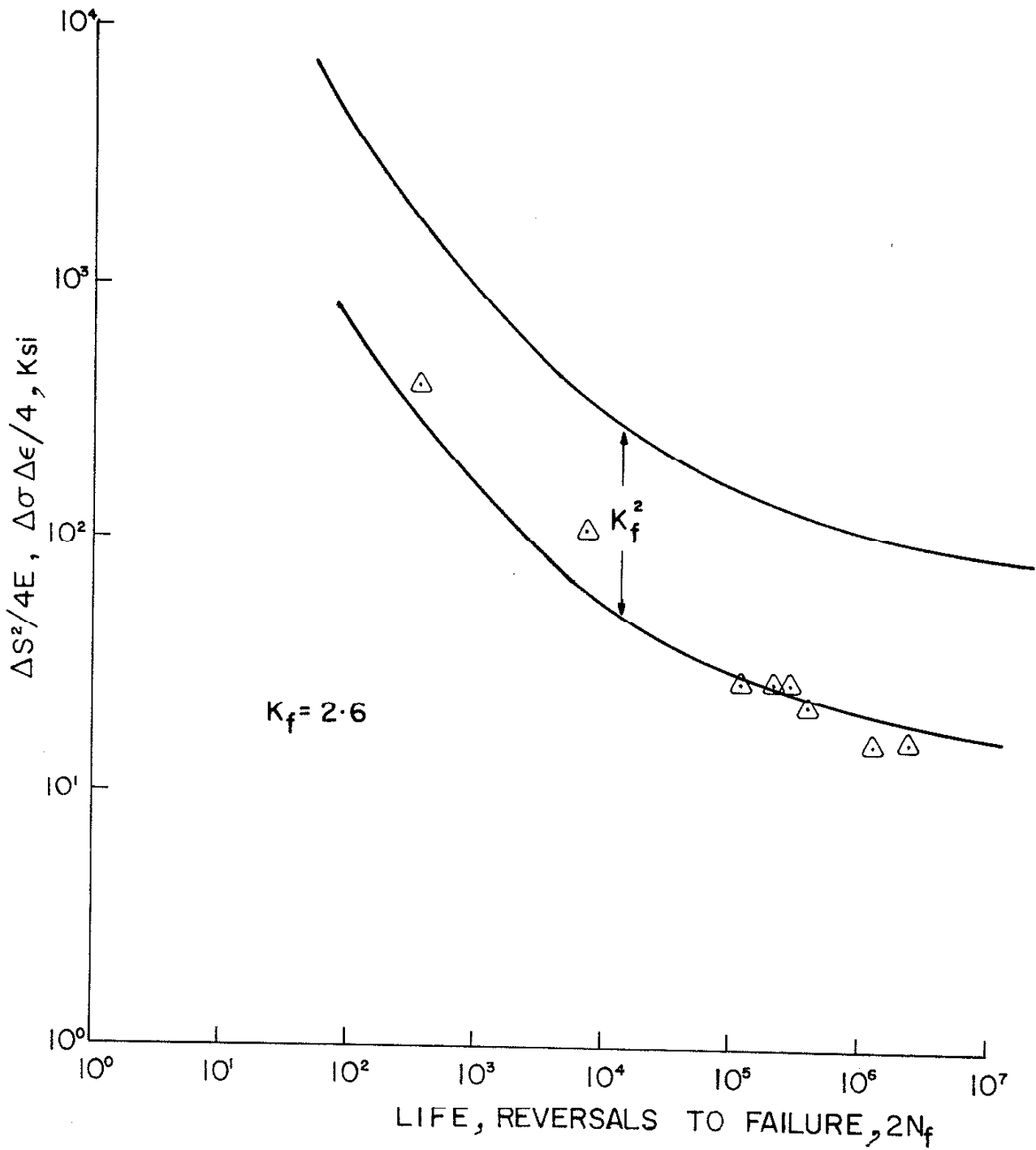


Fig. 32 NEUBER PLOT FOR RQC-100 SPECIMEN

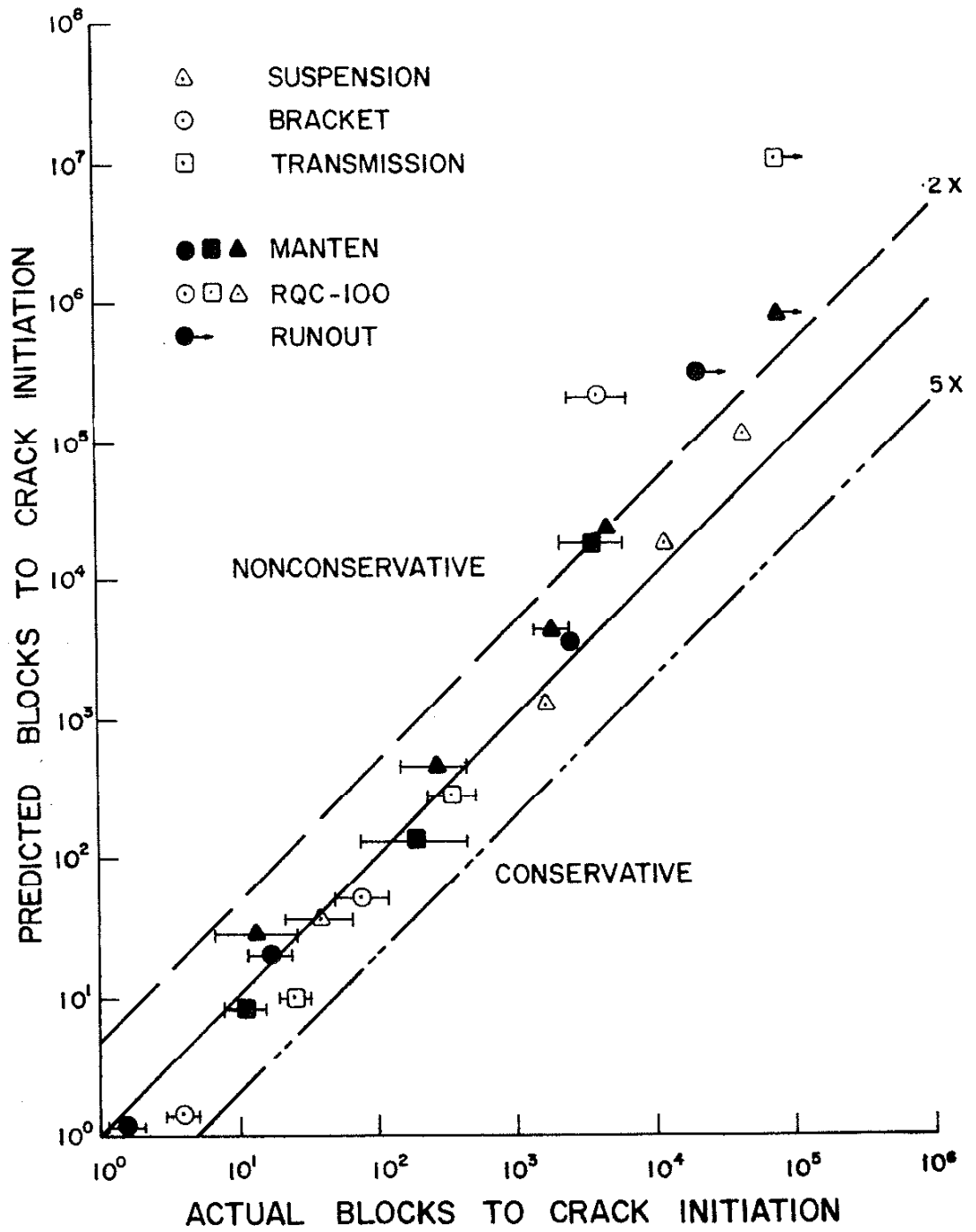


Fig. 33 NEUBER NOTCH ANALYSIS

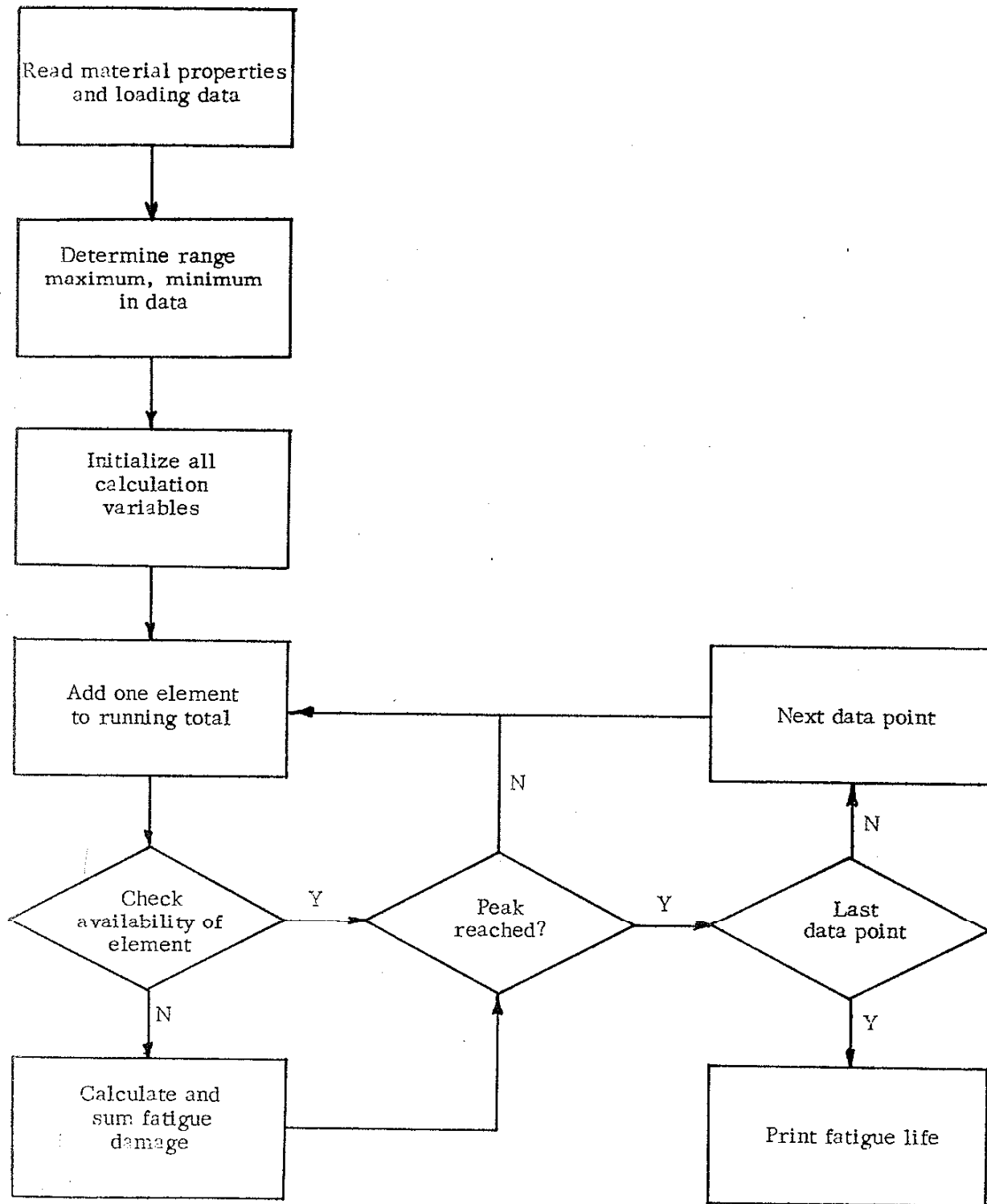


Fig. A1 Overall Flow Diagram

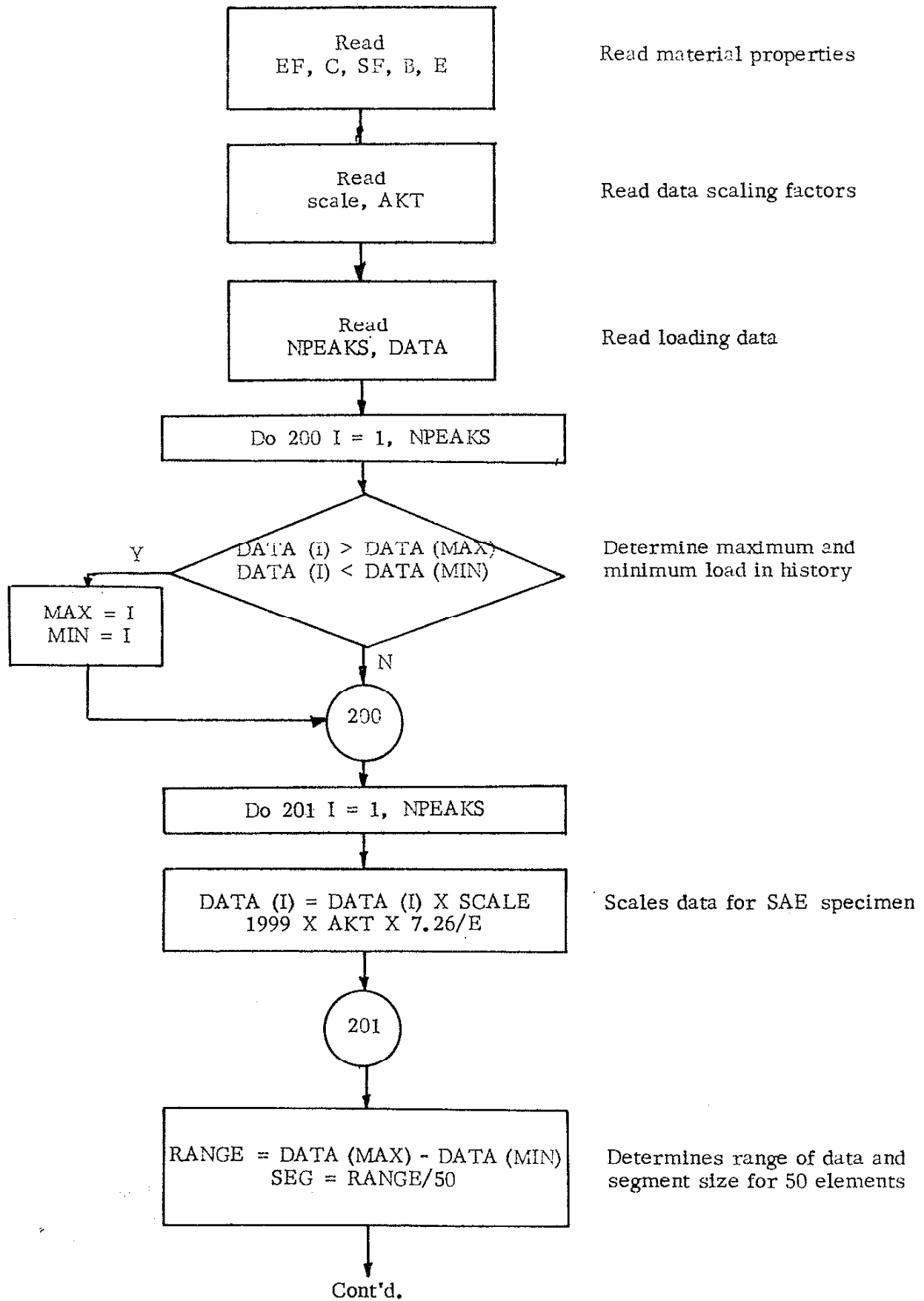
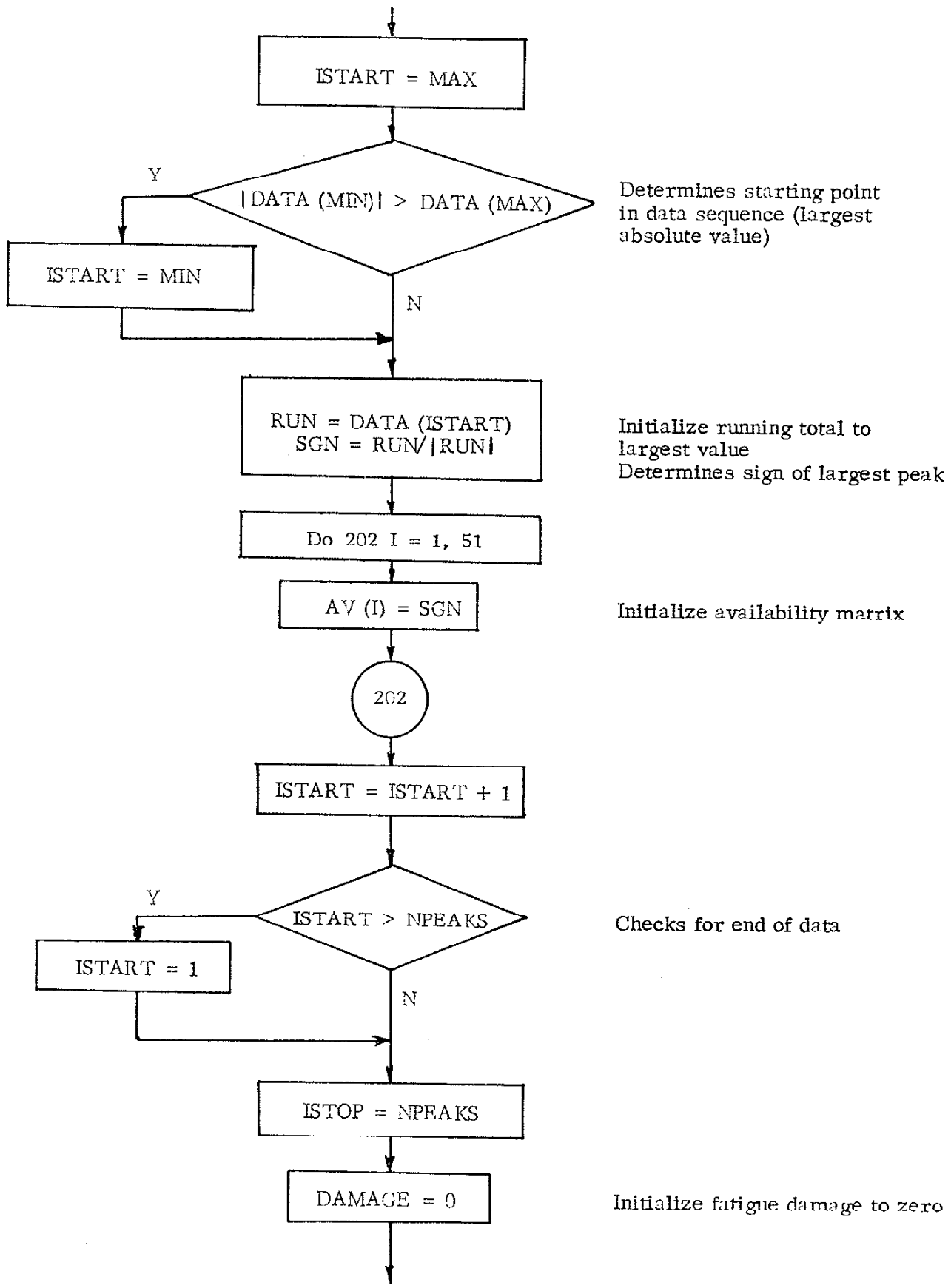


Fig. A2 Detailed Flow Diagram



Cont'd.
Fig. A2 Detailed Flow Diagram

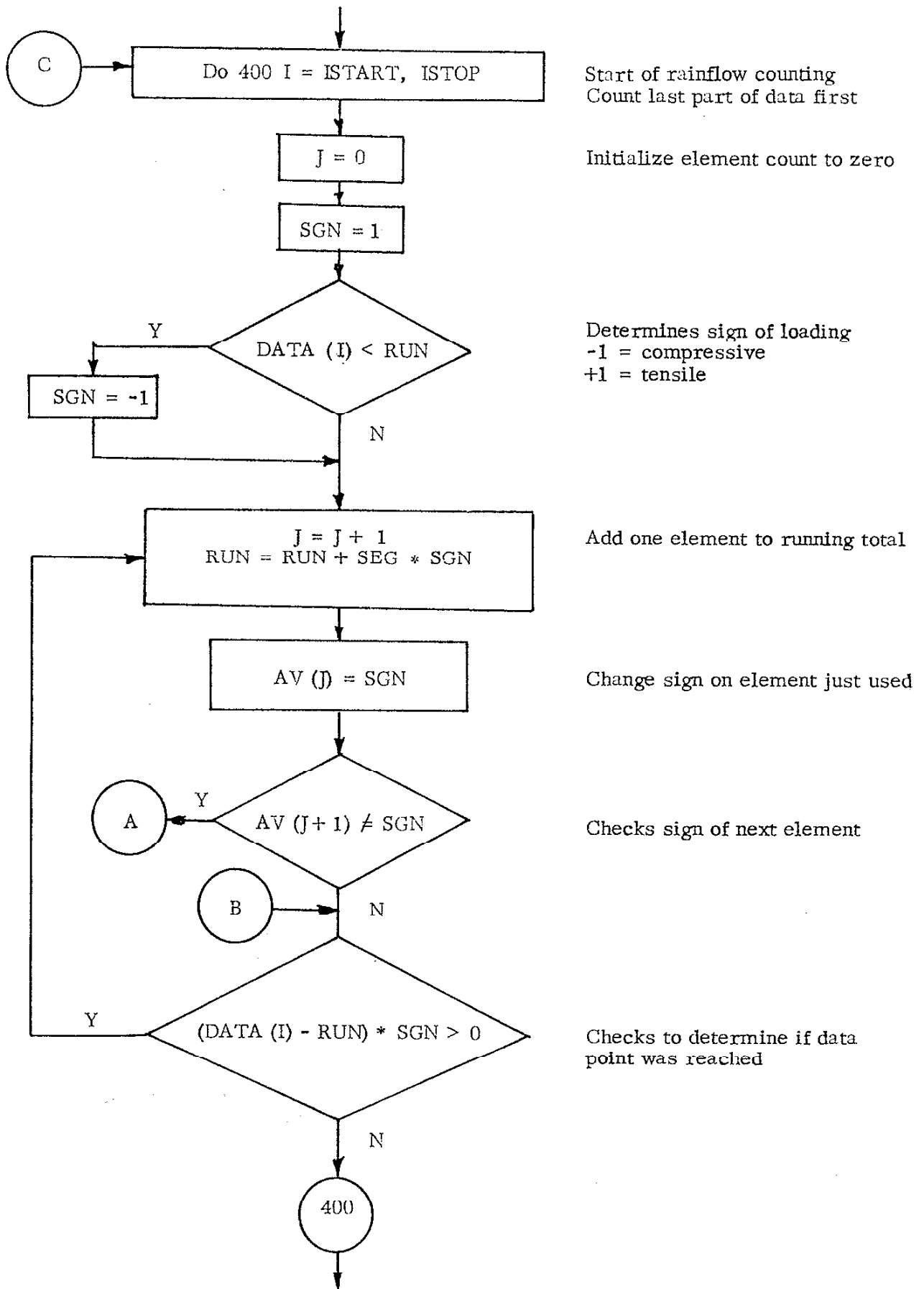


Fig. A2 Detailed Flow Diagram

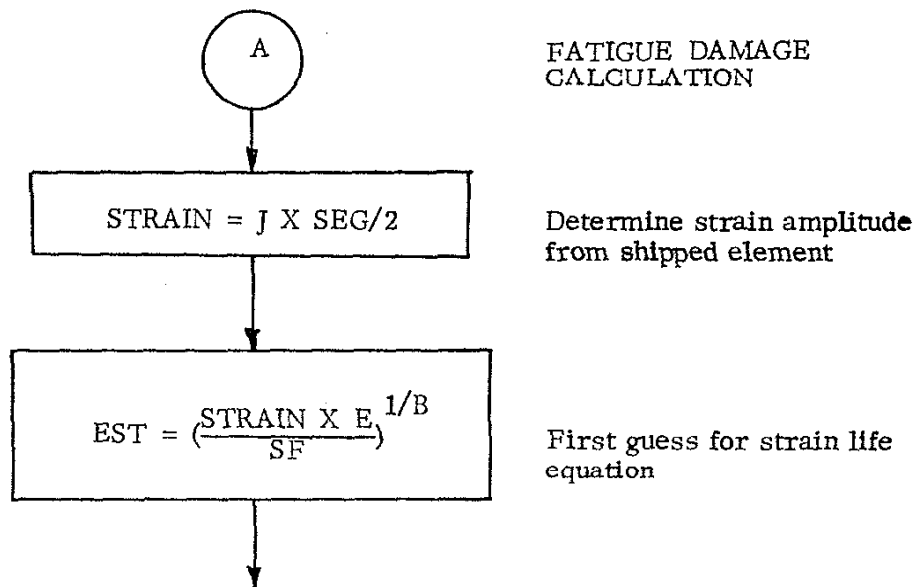
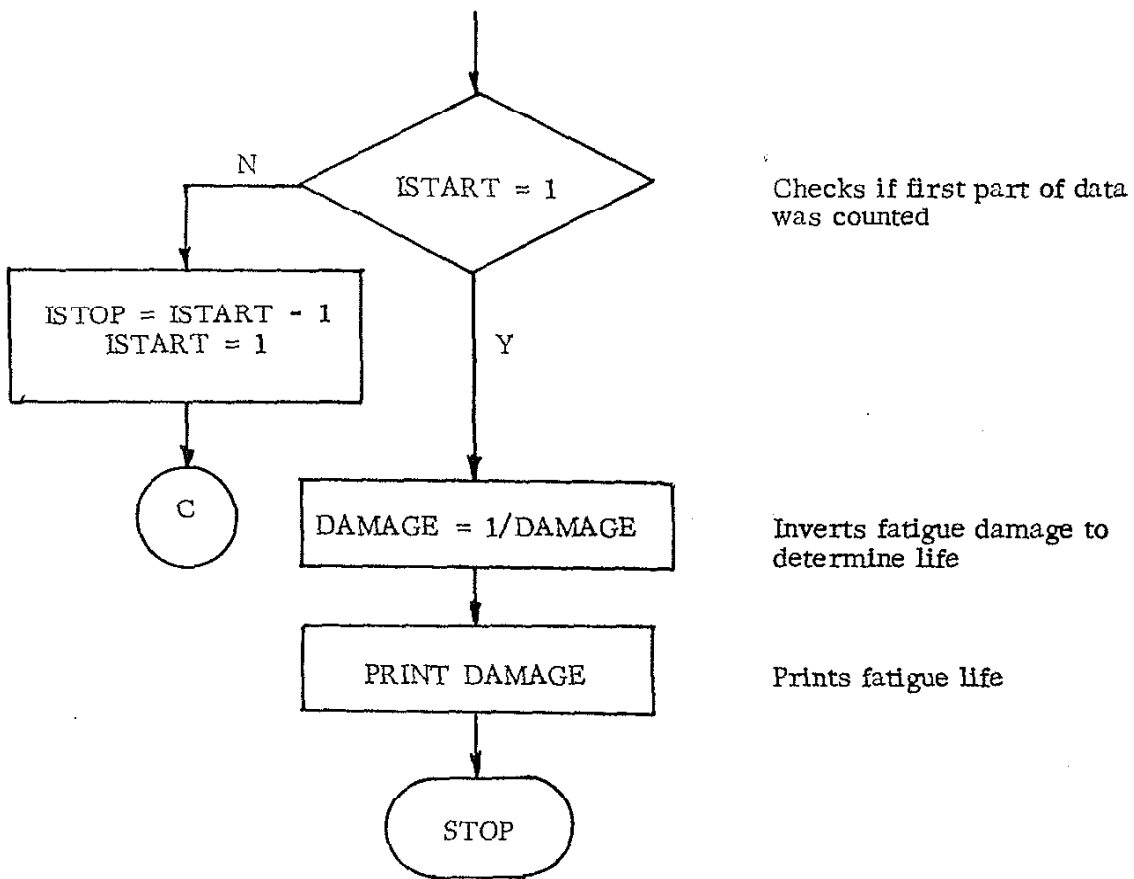


Fig. A2 Detailed Flow Diagram

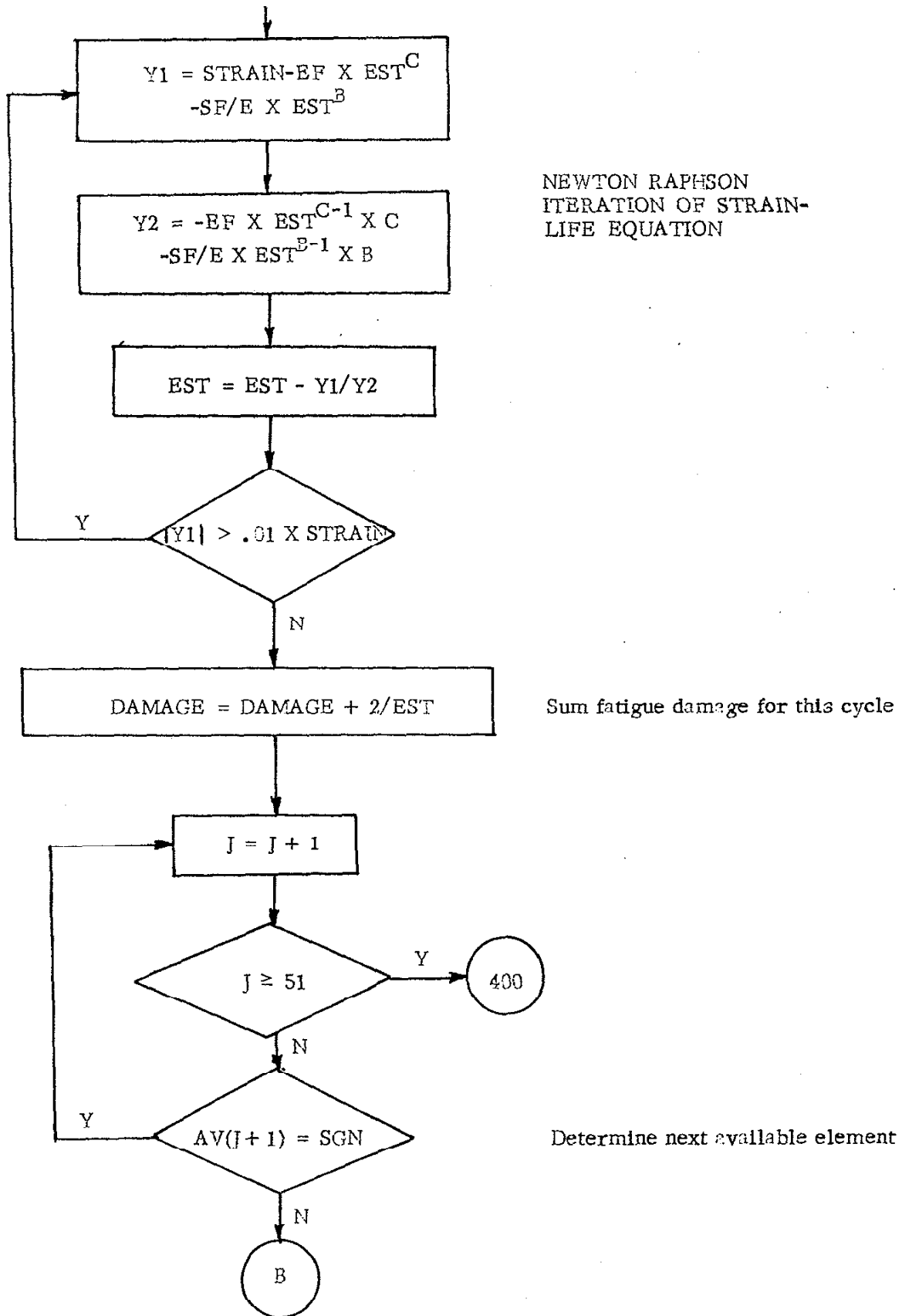


Fig. A2 Detailed Flow Diagram